Severe Local Storms Forecasting*

ROBERT H. JOHNS

National Severe Storms Forecast Center, Kansas City, Missouri

CHARLES A. DOSWELL III

National Severe Storms Laboratory, Norman, Oklahoma

(Manuscript received 11 May 1992, in final form 13 August 1992)

ABSTRACT

Knowledge of severe local storms has been increasing rapidly in recent years as a result of both observational studies and numerical modeling experiments. This paper reviews that knowledge as it relates to development of new applications for forecasting of severe local storms. Many of these new applications are based on physical understanding of processes taking place on the storm scale and thus allow forecasters to become less dependent on empirical relationships. Refinements in pattern recognition and severe weather climatology continue to be of value to the operational severe local storms forecasters, however.

Current methodology for forecasting severe local storms at the National Severe Storms Forecast Center is described. Operational uses of new forecast applications, new "real-time" data sources (such as wind profilers and Doppler radars), and improved numerical model products are discussed.

1. Introduction

Convective storms produce a wide variety of weather phenomena that might be considered "severe" (a hazard to life and property). For purposes of this discussion, however, only those convectively induced phenomena forecast by the Severe Local Storms Unit (SELS) of the National Severe Storms Forecast Center (NSSFC) will be considered. These are:

(a) tornadoes
(b) damaging winds, or gusts $\geq$ 26 m s^{-1} (50 kt)
(c) hail diameter $\geq$ 1.9 cm (3/4 inch)

Doswell et al. (1993) have described present-day forecasting of tornadoes as consisting of two parts: *anticipation of tornadic potential* in the storm environment, and *recognition of tornadic storms* once they develop. This two-part forecasting/observation process also applies to damaging winds and hail. This paper considers only the first part of this forecasting process, focusing on the relationship between the severe local storm and its environment. Since the primary forecast product of SELS is the *severe weather watch* (see Ostby 1993 for a complete description of SELS forecast products), that is the primary topic within this paper. Other SELS forecast products will be mentioned as well, however.

The forecasting process utilized by SELS involves *parameter evaluation, pattern recognition,* and *climatology* (see section 3a in Doswell et al. 1993). The parameter evaluation and, to a lesser extent, pattern recognition components of severe weather forecasting continue to change as more is learned about storm-scale processes and interactions between the storm-scale and the larger-scale environment. Also, climatological knowledge concerning severe local storms is likely to become more refined as specific studies are conducted to develop regional severe weather (e.g., Hirt 1985; Anthony 1988) and parameter-specific (e.g., Lanicci and Warner 1991) climatologies.

To evaluate parameters and detect patterns, both synoptic-scale and mesoscale analysis are essential tools for severe local storms forecasters. The reader is referred to Doswell (1982) for a discussion of those basic analysis techniques utilized in SELS. Since the early 1980s, additional techniques have been developed to take advantage of new, advanced technology and an enhanced understanding of storm processes and their interaction with the environment. These recent techniques and some traditional techniques presented by Doswell will be considered in the following sections.

While climatological knowledge of severe local storm events is useful in the overall evaluation of the severe weather threat, the atmosphere on any given day may not conform to the statistical norm. Severe events can

* A preliminary version of this paper appeared in the preprints of the Symposium on Weather Forecasting, held in conjunction with the 72nd Annual Meeting of the American Meteorological Society, Atlanta, Georgia, in January 1992.

Corresponding author address: Robert H. Johns, NOAA/NWS National Severe Storms Forecast Center, Room 1728 Federal Office Building, 601 East 12th Street, Kansas City, MO 64106.

© 1992 American Meteorological Society

and do occur in all states, at all times of the year, and at all hours of the day. That is one of the reasons for SELS to be in operation 24 h per day, every day. Moreover, by concentrating their attention on severe weather, SELS forecasters are able to provide important guidance to field forecasters in areas of the country where severe local storms are infrequent. If a forecaster is not accustomed to dealing with severe convective events, those events might be an unpleasant surprise on those relatively rare occasions when they do occur.

A review of the history of severe weather forecasting techniques through the mid-1980s has been presented by Schaefer (1986), and interested readers are referred to his work for a historical perspective on the subject. The primary objective of this paper is to review current severe local storm forecasting techniques, with an emphasis on recent major advances in the field. Knowledge gained from observational studies and numerical model simulations will be discussed, and theories and forecast techniques derived from this knowledge will be presented. The importance of new technology in helping to assess the potential for severe local storm development will also be discussed.

2. Severe local storms forecasting philosophy and methodology

SELS *does not* attempt to have a severe weather watch (Ostby 1992) valid for each and every severe weather event. The density of the operational data network, the state of meteorological understanding, and the temporal and areal scale of SELS forecasts do not allow for reasonable accuracy in attempting to forecast all isolated, marginal severe events. Because of this, SELS concentrates its efforts on issuing watches for *significant* severe weather events (i.e., giant hail, strong and violent tornadoes, etc.; see Hales 1988), and *concentrations* of severe weather events [e.g., 20 reports of 2.5-cm- (1-inch) diameter hail across northern Missouri]. Thus, it is expected that isolated, marginal severe weather events will be handled by the local National Weather Service (NWS) offices in the normal course of their warning duties.

The severe local storms forecasting methodology utilized by SELS varies with the time scale of the forecast product (see Doswell et al. 1993 and Ostby 1992 for definitions and details). Preparation of convective outlook forecasts (out to 52 h) primarily involves interpretation and modification of National Meteorological Center (NMC) numerical model forecast products (see section 3). For those outlook forecasts whose valid period begins within 12 h of the scheduled issuance time, some additional adjustments are made based on diagnosis of current synoptic- and subsynoptic-scale trends.

On the 0–7-h time scale, SELS issues three types of products: mesoscale discussions, severe local storm watches (severe thunderstorm and tornado), and status reports (Ostby 1992). These short-term products are primarily diagnostic in nature, and if they are to be timely and accurate, continuous attention to details and trends of "real-time" weather is required (see Doswell 1986a). For example, regional subsynoptic-scale analysis of surface data (the densest operational data network available) is necessary to assess the short-term severe weather threat (Doswell 1982), so surface analysis typically is done each hour. Further, these subjective surface analyses are complemented by parameters derived from the surface data fields. SELS mesoscale forecasters[1] also examine closely remote-sensing imagery from satellite (e.g., Scofield and Purdom 1986), radar (e.g., Burgess and Ray 1986), lightning (e.g., Lewis 1989), and wind profiler (e.g., Leftwich and Beckman 1992) sources to aid in accurate diagnosis of important synoptic and mesoscale features. These data are available at intervals ranging from nearly continuous (lightning) to hourly (profiler winds).

As additional data sources have become available and NSSFC's means of displaying data has improved, status reports and mesoscale discussions have become more timely and detailed in recent years (see Figs. 1 and 2). In addition to their original uses (see Doswell et al. 1993), these messages are now sometimes utilized to alert field offices to a particularly dangerous mesoscale development (e.g., Fig. 1b), or to discuss a localized severe threat when the expected intensity, area affected, and/or time duration is too limited to justify watch issuance (e.g., Fig. 2b).

Although short-term forecasting of severe local storms is primarily diagnostic in nature (Doswell 1986b), the operational numerical weather prediction (NWP) model forecasts also play a role. Typically, at the beginning of a shift, a SELS mesoscale forecaster examines the short-term model forecasts (6, 12, and sometimes 18 h) to determine model trends for those parameters and patterns related to severe local storm development. Used together with the current convective outlook, they help the mesoscale forecaster focus on areas that require more detailed analysis. Other short-term forecast products use combinations of current surface data and model data to assist the forecaster in estimating current parameter values (see section 3).

3. Initiation of deep convection

Almost all severe local storm events are associated with deep convection. To achieve deep convection, there are three necessary ingredients (as described in Doswell 1987):

[1] The term "mesoscale forecasters" is used to signify those SELS personnel filling positions where the primary responsibility is to monitor "real-time" weather conditions and trends continuously and to issue products concerning short-term subsynoptic-scale events when necessary (i.e., mesoscale discussions, severe weather watches, and status reports).

a

```
STATUS REPORT ON WW NR 179

PSBL SVR TSTMS IN OKC AREA AND OVR WASHITA/KIOWA
CNTY ARE MOVG 225/30-35.  TSTMS CONT TO MOV NE IN
RGN OF UPR DIFFLUENCE AND IMPRESSIVE SLY LO LVL FLOW
AS INDCD BY PROFILERS IN NRN AND WRN OK.  AMS RMNS
MDTLY UNSTBL OVR WRN AND CNTRL OK WITH LI/S OF -4 TO
-6.  DVLPMT WWD TO HBR DURG PAST HR AND A HLF IS
PROBABLY RELATED TO STGST LO LVL MSTR ADVCTN AND
MSTR CNVGNC.  DIFFLUENT ZN APRS TO BE LIFTING NEWD
AND RADAR INDCS NEW CONVCTN DVLPG TWD END/PNC.  AMS
IS DESTABILIZING OVR N CNTRL OK AND S CNTRL
KS...WITH -2 LI/S NOW CROSSING INTO KS.  LOW CLD
ENHNCMT INCS MSTR RACING NWD OVR WRN OK INTO DDC
AREA.  LIFT FM WRM ADVCTN INVOF WRM FNT MAY ALSO AID
DVLPMT OF TSTMS FARTHER N.  AREA NNE OF CURRENT WW
IS BEING MONITORED FOR ADDNL WW.  CONT CURRENT WW.

..JUNGBLUTH..  04/26/91
```

b

```
STATUS REPORT ON WW NR 183

WW NR 183 IS NO LONGER IN EFFECT W OF A 35NNW
CNK..30SW SLN..20WNW P28 LN.  OTRW CONT RMNDER OF
WW.

LN OF SVR TSTMS HAS BEEN DVLPG RPDLY FM JUST N OF
CNK SWD TO NR HUT AND JUST E OF P28.  MOST RAPID
DVLPMT HAS BEEN VCNTY CNK.  RADAR AND STLT INDC
STGST TSTM IS OVR SE CLOUD CNTY JUST SE OF CNK MOVG
210/30.  GOLFBALL HAIL WAS RPTD AT 1843Z NR
MINNEAPOLIS KS WITH THIS STORM.  VSB STLT IMAGERY
SHOWS A FLANKING LN OF DVLPG CU FM THIS TSTM SUGG
CONTD INTENSIFICATION.  EXTRAP WD PLACE THIS TSTM
OVR WASHINGTON CNTY KS ABT 30ENE CNK AT 2015Z AND
ENTERING SWRN GAGE CNTY NEB JUST SW OF BIE AT 2115Z.
THIS TSTM HAS POTENTIAL TO PRODUCE TORNADOES AS IT
MOVES INTO LO LVL JET AND MSTR AXES.

OTHER TSTMS HV BEEN INCRG IN INTENSITY OVR KINGMAN
CNTY KS TO THE W OF ICT.  EXPECT THESE TSTMS TO CONT
DVLPG NEWD NR HUT AND JUST N OF ICT NR SFC MSTR
CNVGN CNTR DURG THE NEXT HR.  TSTMS HV BEEN DVLPG
NEWD ACRS OK/KS BDR INTO SUMNER CNTY KS.

..BECKMAN..  04/26/91
```

FIG. 1. (a) Status report issued at 0646 UTC 26 April 1991 discussing the potential issuance of a watch adjacent to the current watch. Contractions are in accordance with Federal Aviation Admin. Handbooks No. 7340.1L and 7350.6E. (b) As in (a) except issued at 1945 UTC 26 April 1991 and discussing a dangerous mesoscale development over north-central Kansas.

(a) a moist layer of sufficient depth in the low or midtroposphere,

(b) a steep enough lapse rate to allow for a substantial "positive area," and

(c) sufficient lifting of a parcel from the moist layer to allow it to reach its level of free convection (LFC).

Since the essential issue in the formation of deep convection is whether or not the LFC will be attained, the question of "sufficiency" in these ingredients is determined by whether or not some parcel can be expected to become positively buoyant through a deep layer. Moisture, conditional instability, and lifting are all necessary and each affects the convective potential in a different way.

To assess the potential for deep convection, a forecaster must be able to diagnose the current thermodynamic structure of the troposphere and to forecast changes resulting from thermal advection, moisture advection, and vertical motion fields. Currently, the diagnosis of these factors is done by means of twice-a-day (0000 and 1200 UTC) radiosondes taken from a network of stations around the world. Radiosondes give the forecaster a snapshot of vertical thermodynamic and wind profiles at widely scattered points. The challenge is to deduce the structure *between* observations in space and time, utilizing the limited sounding data, and to project temporal changes in this structure for the forecast period in question.

In the early days of sounding analysis, forecasters hand plotted local radiosonde data on a thermodynamic diagram (e.g., a pseudoadiabatic chart), and assessed the potential for deep convection graphically, based on expected diurnal heating and other factors. Estimation of static instability (positive area) and cap

a

```
SELS MESOSCALE DISCUSSION FOR ..NRN OH/NWRN PA/WRN
NY..
CONCERNING... SEVERE THUNDERSTORM POTENTIAL

LTG/STLT IMAGERY SHOWS LN OF TSTMS OVR SRN ONT APCHG
YXU MOVG ESEWD 30 KT.  VIS IMAGERY SHOWS DVLPMT SWWD
ACRS EXTREME SERN LWR MI TWDS NWRN OH.  STGST WARM
ADVCTN/VRT MTN FCST BY MRNG PROGS TO BE ACRS PTNS OF
WRN NY/SERN ONT BY 00Z.  INCRG SFC PRES FALLS ACRS
WRN NY/NWRN PA REFLECT ONGOING WRM ADVCTN PAT.  CI
SHEILD HAS LIMITED DEGREE OF SFC HEATING ACRS WRN
NY/WRN PA/NRN OH...BUT AMS HAS BCM MDTLY UNSTBL WITH
SFC-BASED LI/S IN THE -5 TO -7 RANGE.  EXPC
ADDITIONAL DVLPMT/INTENSIFICATION OF TSTMS OVR SRN
ONT/NWRN OH NEXT 2-3 HRS...AND AREA FM NRN OH THRU
NWRN PA INTO WRN NY IS BEING CLOSELY MONITORED FOR
PSBL WW.

..HIRT..  07/22/91
```

b

```
SELS MESOSCALE DISCUSSION FOR  ..SE VA/ERN NC..
CONCERNING... SEVERE THUNDERSTORM POTENTIAL

STLT/RDR DATA INDC TSTMS HAVE INTSFYD ACRS SE VA/ERN
NC SINCE 0930Z AS ERYR INTS SQLN HAS ENCOUNTERED
MDTLY UNSTBL AMS.  SFC DEWPTS HAVE RISEN INTO THE
MID/UPR 60S FM THE NKT/EWN AREAS NWD THRU ORF AND
INTO THE VA/MD ERN SHORE ON THE HEELS OF STG SLY LO
LVL FLOW.  STMS ARE INCRG ALG TAIL END OF STG SHRTWV
TROF ROTG THRU THE CAROLINAS/MID ATLANTIC RGN ATTM.
PRES FALL/RISE COUPLET ASSOCD WITH SQLN CONTS TO BE
WELL DEFINED AND SUGS CURRENT ACTVTY WILL REMAIN
ORGANIZED AS IT MOVES EWD/NEWD 30-35 KTS TWD THE
ATLC CST.  STGST CELLS WITHIN LN ARE CURRENTLY
EXHIBITING LEWP/BOW ECHO TYPE RADAR CONFIGURATIONS.
THUS...XPC ISOLD TSTMS WILL PRODUCE WINDS NR SVR
LVLS AND PSBLY SOME SMALL HAIL AS THEY AFFECT THE
WAL/ORF/ECG/EWN/NKT/HAT AREAS OVR NEXT 2-4 HRS.

..SAMMLER..  03/02/91
```

FIG. 2. (a) As in Fig. 1a except for mesoscale discussion issued at 1829 UTC 22 July 1991 discussing synoptic and subsynoptic scale conditions and trends that may lead to a watch issuance. (b) As in (a) except issued at 1045 UTC 2 March 1991 and discussing a small area where the severe threat is likely to be limited in duration.

(negative area) were an important part of this process. Since technology at that time did not allow for timely quantitative determination of positive and negative areas, several stability indices (e.g., the SELS lifted index; Galway 1956) were developed. Such indices, many of which remain in use today, key primarily on mandatory pressure-level data. This makes them sensitive to the details in the sounding and, hence, they may be unrepresentative of the true character of the data. Further, the sounding used in their calculation can change significantly in the time between the sounding and convective development, so the numerical values can be unrepresentative in this way, as well. As technology and our understanding of storm processes have changed, new techniques and parameters are evolving that make use of more of the information in a sounding than the traditional indices. Currently at SELS, forecasters use the VAS [VISSR (Visible and Infrared Spin Scan Radiometer) Atmospheric Sounder] Data Utilization Center (VDUC) interactive computer system (Browning 1991, 1992) routinely to display thermodynamic profiles and to determine derived parameters. Local analysis computer programs, such as CONVECT (Stone 1988), and interactive programs, such as the Skew T–log$p$/Hodograph Analysis and Research Program (SHARP; Hart and Korotky 1991), are being utilized widely by local forecasters to assist in quantitative sounding analysis. These interactive programs incorporate the old indices along with newer ones (e.g., convective available potential energy, or CAPE) and allow the forecaster to modify the sounding data to attempt to account for anticipated spatial and temporal variations in the storm environment.

To assist the SELS forecaster in defining (in both area and time) the short-term potential (0–7 h) for thunderstorm development, hourly surface data are used to compute parameter fields, some of which are modified for expected changes aloft.[2] By this means, the forecaster can obtain hourly estimates of such parameters as surface parcel lifted index values (positive area), cap strength (negative area), low-level convergence (implying localized lifting, usually along a boundary; see, e.g., Wilson et al. 1988), and many others.

Forecasting for the longer term (e.g., the SELS 0700 UTC convective outlook forecasts the potential for general thunderstorms for a period extending out to 29 h from issue time) primarily involves interpretation of numerical model products. Typically, the SELS forecaster constructs a *composite chart* of "initial" conditions as soon as data from the latest radiosonde release have been analyzed (see Doswell 1982, II 31–32). From this composite chart, the three-dimensional relationships among the "initial" synoptic patterns and meteorological parameter fields can be visualized.

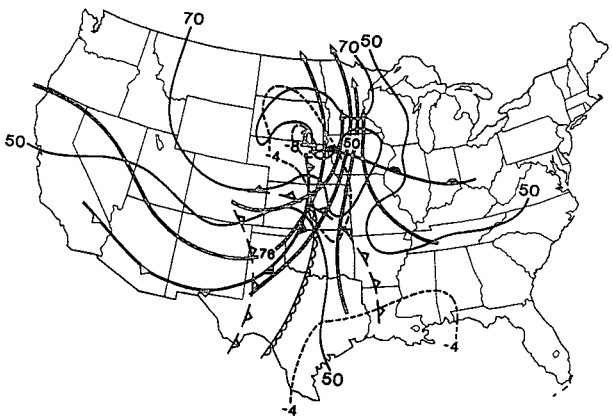

FIG. 3. An example of a composite prognosis depicting 12-h forecast positions of those surface and upper-air parameters that affect severe thunderstorm development. Forecast is for 0000 UTC 27 April 1991 based on initial data from 1200 UTC 26 April 1991. This is a black-and-white copy of a color original in Doswell et al. 1993 (their Fig. 1); the details of the parameter coding can be found therein and are not important here. Rather, the intent here merely is to exemplify the appearance of a composite prognosis.

Composite *prognoses* ("progs") for 12-h intervals out to 48 h from the time of the "initial" composite chart (Fig. 3) are then constructed, primarily by assimilating NWP model products from the NMC. Patterns and parameter values on the resultant prog charts are utilized to prepare forecasts both for deep convection and for severe weather events (see sections 4, 5, and 6). Concerning deep convective development, model parameters that relate to such factors as vertical motion, instability (positive area), and the capping inversion (negative area) are included on the prog charts. Recently, a procedure was developed at NSSFC that allows the forecaster to display many of the operational NWP fields used in constructing composite progs (Cope 1992). The procedure assigns a particular color to each parameter field and has a looping capability that allows the forecaster to see how model forecast fields change with time. Any combination of fields may be superimposed (e.g., instability and vertical motion; Fig. 4).

Another important notion in developing the forecasts is that of *limiting factors*. Limiting factors allow the SELS forecaster to refine his/her perception of where deep convection is possible. The following are some examples.

1. Deep convection is usually limited to those areas where the NGM forecast 1000–500-mb mean relative humidity is greater than 40% to 45%.

2. Deep convection is generally limited to those areas where lifted index values [from combined use of

[2] For example, VDUC uses 500-mb static temperatures to compute surface-based lifted index values for the first few hours after receipt of scheduled radiosonde data, with Nested Grid Model (NGM) forecast 500-mb temperatures being used when they become available (4 to 9 h after scheduled radiosonde data receipt).

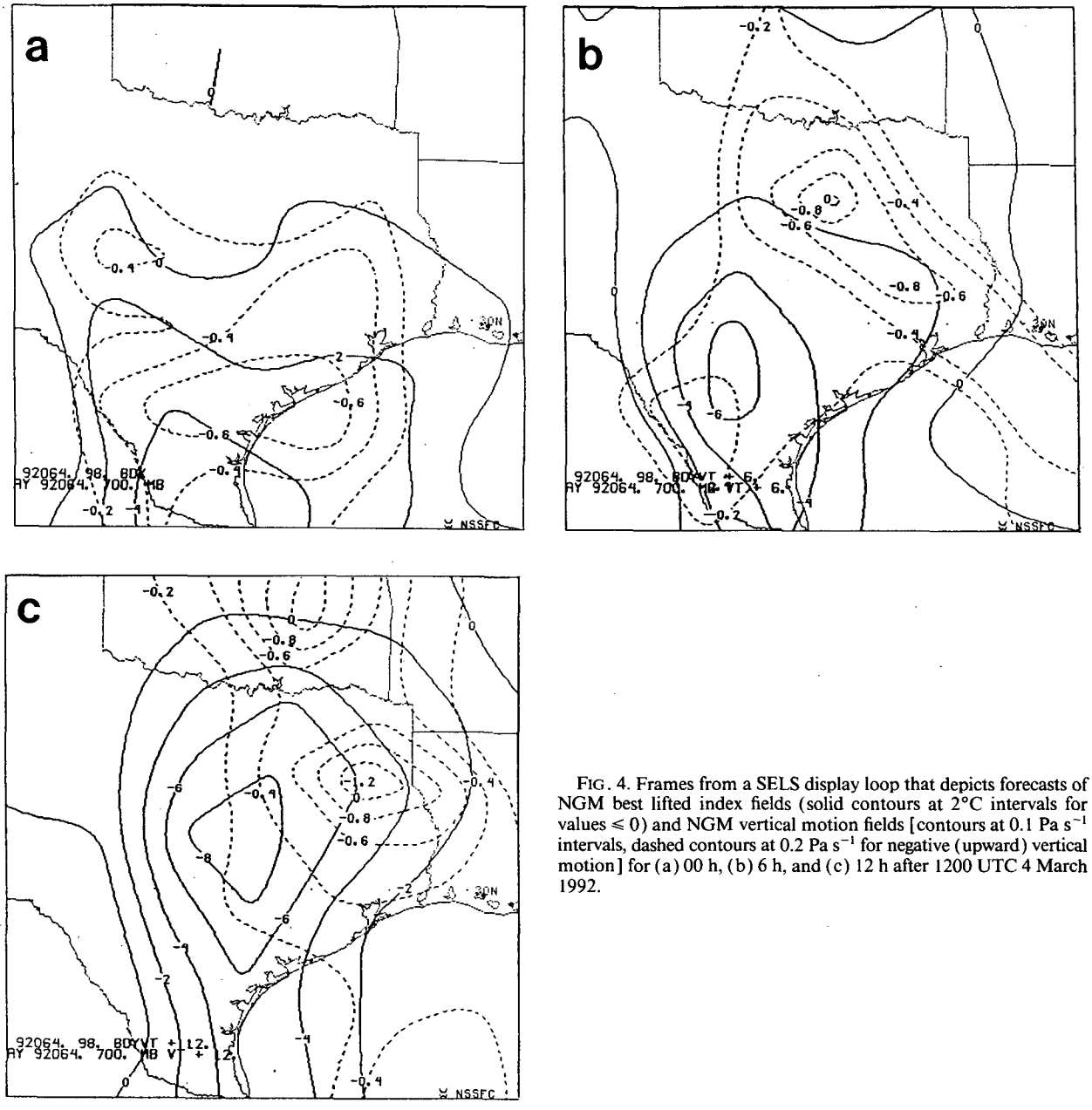

FIG. 4. Frames from a SELS display loop that depicts forecasts of NGM best lifted index fields (solid contours at 2°C intervals for values ≤ 0) and NGM vertical motion fields [contours at 0.1 Pa s^{-1} intervals, dashed contours at 0.2 Pa s^{-1} for negative (upward) vertical motion] for (a) 00 h, (b) 6 h, and (c) 12 h after 1200 UTC 4 March 1992.

the Limited-area Fine-mesh Model (LFM) and NGM output, and computed surface parcel lifted index values] are zero or less. Since the NGM often does not forecast thermodynamic profiles accurately (particularly boundary-layer moisture), model prediction of lifted index values is frequently "poor" (see Weiss 1987a). The SELS forecaster uses a combination of the most reliable aspects of both the NGM and LFM forecasts of lifted index values and patterns in preparing composite prognoses. Another method of making lifted index forecasts is to compute surface parcel lifted index values (Hales and Doswell 1982) for specific points of interest. The technique requires an estimate (or observation) of surface temperature and dewpoint at a particular place and time, along with a forecast 500-mb temperature (say, from the NGM) valid for the same place and time. It should be noted that using surface-based values for determining lifted index can be unrepresentative; for example, there may be a shallow stable layer near the surface, above which lies a deep, unstable layer. However, in spite of this limitation of a surface parcel lifted index, the result usually is more representative than the NGM forecast lifted index value.

3. Deep convection is usually limited to those areas where the forecast 700-mb temperature (NGM) is colder than 12°C. Deep convection also generally is limited to areas where the forecast 1000–500-mb thickness values (NGM) are 5790 m or less. These two empirical rules relate to the strength of the low-level capping inversion (between 850 and 700 mb) or "negative" area. They do not apply at high surface elevations (e.g., where 700 mb becomes a part of the mixed layer), and such a strong cap still may be overcome in certain situations, such as when convection develops above the cap.

4. Deep convection is usually limited to areas where the NGM-forecast 700-mb vertical motions are generally neutral (> -3 to $< +3 \times 10^{-3}$ mb s^{-1}) to decidedly upward ($< -3 \times 10^{-3}$ mb s^{-1}; note that the sign is reversed on NGM output). This relates primarily to the effects of synoptic-scale vertical motion on the strength of the capping/subsidence inversion. In some cases, however, this limiting factor may also be related to mesoscale and smaller-scale lifting mechanisms that allow a parcel to reach its LFC. NWP model forecasts for low-level boundaries and maxima in low-level moisture convergence are more reliable indicators of such small-scale processes than the model's vertical motion, per se.

It should be noted that although the forecaster extracts many of the limiting factors directly from NGM fields when preparing a composite prognosis chart, the actual convective forecast often must be adjusted to account for perceived model biases (Junker et al. 1989). Further, for those outlooks that become valid within 12 h from the time of issuance, a close assessment of the synoptic- and subsynoptic-scale initial conditions and trends in surface and upper-air features is made prior to forecast issuance (Doswell 1986a). This typically includes examining most "real-time" data sources (e.g., satellite imagery) and subjectively analyzing a surface chart covering all areas of interest. Significant differences between model trends and real-time trends are noted and the forecast is adjusted accordingly (e.g., Hales 1979), particularly in the case of ongoing deep convection. In such situations, shallow baroclinic boundaries often develop that may disrupt the flow of low-level moisture from the source region. Such mesoscale developments can dramatically affect the convective evolution over a broad region.

Recently, NMC-generated model forecast soundings (Plummer 1989) have become available. For selected cities across the continental United States, the forecaster can display model forecast thermodynamic and wind profiles at hourly intervals out to 48 h, showing how key elements in the *model* atmosphere change with time (e.g., changes in the cap strength or the depth of the moist layer). Of course, these soundings are only as good as the model forecast, and have relatively coarse vertical resolution (16 levels). Since systematic biases are present in models, model sounding data may need subjective adjustment using computer programs like SHARP (Hart and Korotky 1991). For example, low-level moisture can be added to the model-forecasted boundary-layer conditions in situations where experience with the NWP models suggests a dry bias. The forecaster then can see quantitatively how this change would affect parameters derived from the modified sounding.

NSSFC recently gained the ability to modify model forecast thermodynamic profiles using hourly surface data (Bothwell 1992). The thermodynamic profile for the surface lifted parcel is overlaid with the model forecast profile, so that positive and negative areas can be visualized (see Fig. 5a). This diagnostic tool has been helpful to SELS forecasters in making short-term forecast decisions.

Once the forecaster decides that deep convection is likely, the next question is whether or not this convection will be capable of producing large hail, damaging winds, or tornadoes. That is, the forecast task shifts from forecasting deep, moist convection to forecasting severe convective weather, which clearly is contingent on the presence of deep convection.

4. Forecasting large hail

Hail development is quite complex, and the reader is referred to Knight and Squires (1981) and Morgan and Summers (1986) for additional information. A necessary ingredient for development of large hail is a strong updraft—that is, one that is capable of supporting the weight of a hailstone long enough for it to reach a large size. A primary contributor to a strong updraft is thermal buoyancy (positive area) for lifted parcels. In general, the greater the buoyancy, the greater the potential for large hail. Over the years, this relationship has been a primary factor used in computations to estimate potential hailstone size at ground level from radiosonde data (e.g., Fawbush and Miller 1953; Foster and Bates 1956).

Updraft strength, by itself, is not a sufficient indicator that large hail will develop. Hail development and size attained appear to be greatly affected by variations in storm-scale wind structures (see Nelson 1983). These variations affect the transit time of hail embryos through the hail-growth zone. Because of these variations in structure, supercells (or strong multicell storms) occurring in similar thermodynamic environments may differ in the size, amount, and distribution of hail produced.

Another important factor affecting hailstone size at the surface is the effect of melting as hailstones fall through the freezing level to the surface. Melting is influenced by a number of subfactors, including 1) distance between the freezing level and the ground, 2) mean temperature of the downdraft air between the hailstone's freezing level and the ground, and 3) hail-

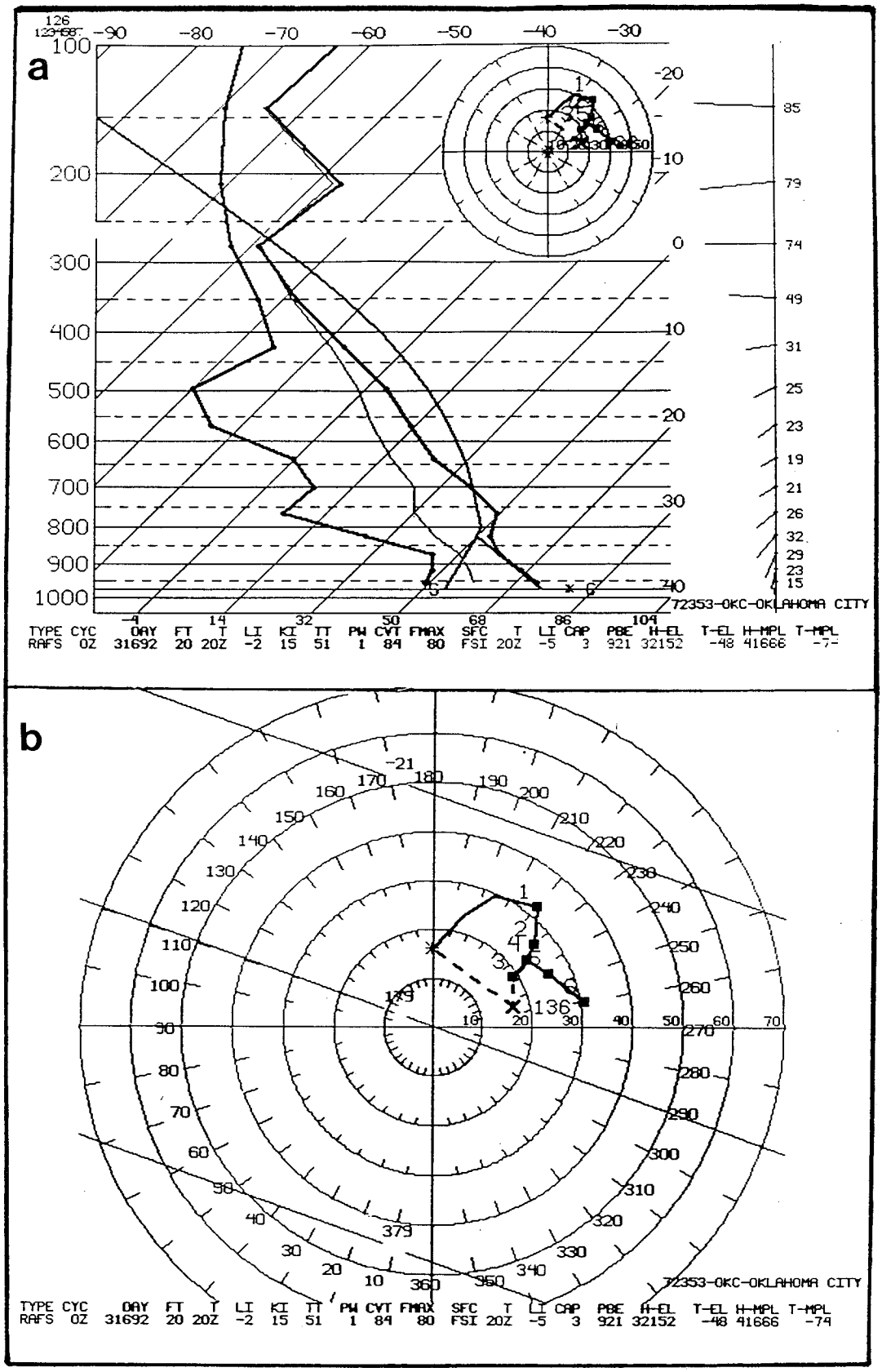
a
b
72353-OKC-OKLAHOMA CITY
TYPE CYC DAY FT T LI KI TT PW CVT FMAX SFC T LI CAP PBE H-EL T-EL H-MPL T-MPL
RAFS 0Z 31692 20 20Z -2 15 51 1 84 80 FSI 20Z -5 3 921 32152 -48 41666 -74

stone size, which affects how long it takes the hailstone to fall.

The environmental wet-bulb zero (WBZ) level approximates the freezing-level height of downdraft air, within which the hailstone is likely to be found. The higher this level is, the longer the melting process can operate. Also, the higher the mean temperature between the WBZ level and the ground, the faster the melting rate. Large hailstones fall at greater terminal velocities than small stones; that is, for a given WBZ level, melting of small hailstones lasts for a longer time than it does for larger stones. Moreover, melting takes place on the surface of the stone and surface area is proportionately greater for small stones than for large stones; area goes up as the *square* of the radius whereas volume goes up as the *cube* of the radius. Attempts to account for melting effects are included in the hail-size algorithms discussed earlier. Together with the updraft component (due to buoyancy), they make up the major components of these algorithms.

Another factor influencing hail development not accounted for by these algorithms is the nonhydrostatic pressure effects on updraft strength. Numerical simulations (e.g., Weisman and Klemp 1984; Brooks and Wilhelmson 1990; McCaul 1990) strongly suggest that interaction of the updraft with environmental winds can create perturbation pressure gradients and resultant vertical accelerations that contribute substantially to updraft speeds. In some instances, this contribution may be *more* influential than buoyancy in driving the updraft (Weisman and Klemp 1984; McCaul 1990). Since the environmental wind structure associated with these vertical accelerations also is associated with supercell development (see section 6), the effects would apply particularly to supercell convection. Therefore, forecasters should remember that when supercells (or strong, well-organized multicells) are present, hail sizes may be considerably larger than the current operational algorithms would predict.

When employed operationally, the traditional methods of estimating hail size (e.g., Fawbush and Miller 1953; Prosser and Foster 1966) have resulted in, at best, limited success (e.g., Doswell et al. 1982). Part of the problem with these algorithms is that they are based on soundings taken from a widely spaced network at relatively infrequent (12 h) intervals. Therefore, their input data may not be representative of conditions when convective storms develop. Leftwich (1984) has shown that, using the algorithm of Foster and Bates (1956), the reliability of its predicted sizes deteriorates rapidly as time advances past sounding release time.

Recently, Moore and Pino (1990) introduced a hail-size forecasting algorithm that accounts for the negative effects of water loading and entrainment on the strength of the updraft. It is designed to be used in an interactive manner, with hail-size forecasts adjusted using advected temperatures aloft and the latest surface data. In preliminary tests by Moore and Pino involving cases from the plains region during the summer, this algorithm has shown significantly greater skill in forecasting hail size than that of Fawbush and Miller (1953).

Supercells associated with relatively weak instability often do not produce large hail (Johns and Sammler 1989). Operational experience suggests that such occurrences are most common from late fall through early spring, in the region from the lower half of the Mississippi valley to the southeastern United States. As an example, during the Raleigh, North Carolina, tornado outbreak of 28 November 1988, no large hail [diameter 1.9 cm (3/4 inch) or greater] was reported from any of the three supercells that tracked across portions of North Carolina and Virginia (STORM DATA 1988; and personal communication with R. Gonski from the NWS Forecast Office in Raleigh). Empirically, it seems that the current hail-size forecasting algorithms perform best in "pulse" storm environments. The complexity of hail development with more organized convection suggests that attempts to develop a forecasting algorithm that is effective in supercell and strong multicell environments (see sections 5 and 6) may be a difficult task.

While forecasting for severe weather watches is focused on hail-size estimation algorithms, for SELS convective outlooks, both pattern recognition and climatology play a role. An example of a pattern typically associated with hail is the "cold low" pattern (Type D in Miller 1972). When moisture is sufficient for moderate to strong instability in the vicinity of the cold pool aloft associated with an upper closed low, relatively low-topped thunderstorms are likely during afternoon and early evening hours. Hail often is reported with this convection and, if instability is sufficient, hail diameters can exceed severe limits. Hail diameters in these situations rarely exceed 4.4 cm (1 3/4 inch). In cold low patterns, the common occurrence of hail at

FIG. 5. (a) The 0000 UTC 16 March 1992 NGM forecast sounding for Oklahoma City, Oklahoma (OKC), at 2000 UTC 16 March and the actual 2000 UTC surface-based lifted parcel thermodynamic profile for Fort Sill, Oklahoma (FSI) (medium line). The NGM forecast sounding shows the thermodynamic profile (heavy line), wet-bulb temperature (light line), hodograph (upper right), and a wind profile (on right; wind speeds in knots, with flag indicating direction and length of flag proportional to speed). An explanation of other parameters may be found in Bothwell (1992). (b) Magnification option for hodograph in (a); numbered squares on hodograph indicate height (AGL) in km. The first point of the hodograph represents actual 2000 UTC surface wind at FSI. The X indicates storm motion vector as estimated by multiplying the 0–6-km AGL mean wind speed by 0.75 and using a direction 30° to the right of the 0–6-km AGL mean wind direction (denoted by 30R75).

the surface is aided by low WBZ heights and low mean temperatures below the WBZ height.

An example involving climatology can be found in late spring and summer over the central High Plains (Kelly et al. 1985). If moderate to strong lapse rates and moisture, resulting in moderate to strong instability, are forecast in an upslope flow severe thunderstorm pattern (Doswell 1980), large hail is very likely to be associated with any strong storms that develop. Therefore, in those upslope flow cases where parameters (other than instability) supporting severe thunderstorm development are forecast to be marginal, but instability is expected to be moderate to strong, the forecaster may predict a risk of severe thunderstorm development in the outlook, based solely on the regional climatological association of those conditions with large hail.

5. Forecasting damaging winds

Damaging straight-line winds associated with deep convection almost always are generated by outflow that occurs at the base of a downdraft.[3] Fujita and Byers (1977) designated exceptionally strong downdrafts as *downbursts,* but the term's meaning has grown to encompass any damaging (or potentially damaging) winds produced by downdrafts. Fujita (1978) has noted that damaging windstorms can occur on different scales, and has called special attention to the *microburst,* which he defines to be a downburst $\leq$ 5 km in diameter.

Given that deep convection develops (see section 3), ingredients necessary for damaging winds at the surface are those promoting strong downdrafts. *Precipitation loading* and *negative buoyancy due to evaporative cooling* are recognized factors in initiating and sustaining a downdraft (Doswell 1982). Precipitation loading is the drag effect of liquid water, which enhances parcel descent. Essentially, the greater the quantity of liquid water per unit volume, the greater the precipitation drag.

The other factor, negative buoyancy due to evaporative cooling, is created when precipitation falls through a layer of unsaturated air. Once a downdraft is established, continued entrainment of unsaturated air can aid evaporation. Studies indicate that most of the entrained air originates from middle layers of the atmosphere (approximately 3–7 km AGL; e.g., see Foster 1958). Generally, downdraft strength is enhanced by availability and entrainment of relatively dry (low relative humidity) air.

Evaporative cooling (and downdraft strength) also is enhanced by 1) large liquid water content per unit volume, 2) small drop size, and 3) a steep lapse rate, as noted by Kamburova and Ludlam (1966) and Srivastava (1985). The large liquid water content and drop-size factors relate to the amount of liquid water surface available for evaporation. Further, a steep lapse rate acts to maintain negative buoyancy as a downdraft parcel descends.

Downward transfer of horizontal momentum from strong flow aloft can enhance outflow (Brandes 1977 and others). Generally, the stronger the environmental winds in the downdraft entrainment region, the greater the potential contribution to outflow strength. It is unclear how much of this contribution actually is realized in outflow wind speeds (see Foster 1958), however.

From the viewpoint of convective wind-gust forecasting, it is important to distinguish between updraft and downdraft instability. *Updraft* instability invariably is associated with *positive* buoyancy created by the temperature difference between a parcel rising moist adiabatically and its environment. Thus, moisture is necessary to ensure that ascent is along a moist adiabat, while high lapse rates create a large temperature difference between the parcel and the environment. The drag from water loading tends to *diminish* the effects of positive buoyancy.

Downdraft instability, on the other hand, is primarily the result of *negative* buoyancy. In downdrafts, the drag from water loading combines with the effects of negative buoyancy to *enhance* downdrafts. Whereas virtually all unstable updrafts are saturated, unstable downdrafts may or may not be saturated. If a parcel descends unsaturated, a high lapse rate is required; if a parcel descends saturated, there must be a continuous source of liquid water for evaporation. Otherwise, the parcel quickly will become warmer than its environment through adiabatic heating, thereby retarding its descent. Conditions for unstable downdrafts, therefore, do not necessarily coincide with those for unstable updrafts. Those indices and parameters that reflect updraft instability will not necessarily be reliable indicators of downdraft instability.

Early algorithms developed to predict outflow speeds (e.g., Fawbush and Miller 1954; Prosser and Foster 1966) attempted to account for negative buoyancy created by evaporative cooling and for momentum transfer. Their success has been limited, however, for reasons similar to those associated with the early algorithms for forecasting hail size (see Doswell et al. 1982). A more recent algorithm by Anthes (1977) accounts for entrainment into the downdraft as an additional component affecting evaporative cooling. Pino and Moore (1989) have developed an algorithm used interactively that combines Foster's (1958) ideas about outflow strength with Anthes' ideas about entrainment. The Pino–Moore wind-gust forecasts are adjusted with time using advected thermodynamic parameters aloft and the latest hourly surface data. In preliminary testing, the algorithm shows an increase in skill over those of Fawbush and Miller (1954) and Prosser and Foster (1966).

[3] On some rare occasions, *inflow* winds can attain damaging proportions. This is usually restricted to supercells, described in section 6.

a. Wind gusts in weak shear environments

When the environmental shear is weak, the thermodynamic profile (pattern) is a primary signal for identifying when strong convectively induced winds are likely to occur. Two prototypical thermodynamic profiles associated with strong outflow in weak environmental wind situations are 1) the "inverted V" or "Type A" profile (Beebe 1955; Barnes and Newton 1986), and 2) the weakly capped "wet microburst" profile (Read 1987).

The inverted V profile is characterized by a deep dry-adiabatic layer from near the surface to the midlevels, a very dry lower layer, and a moist midtropospheric layer (Fig. 6a). "Dry" microbursts (Krumm 1954; Caracena et al. 1983; Wakimoto 1985) are typically associated with very high LFCs and only marginal instability for updrafts. Thus, convection is usually weak and pulselike in character, and electrical activity may be absent. Because such events usually occur in rather stagnant synoptic conditions, forecast schemes have been developed by Wakimoto (1985) and Caracena et al. (1983) based on 1200 UTC sounding analyses and expectations for diurnal heating. Forecasters have had success in employing such schemes in the wording of their afternoon and evening forecasts (see Sohl 1987) and they are considered in SELS operations.

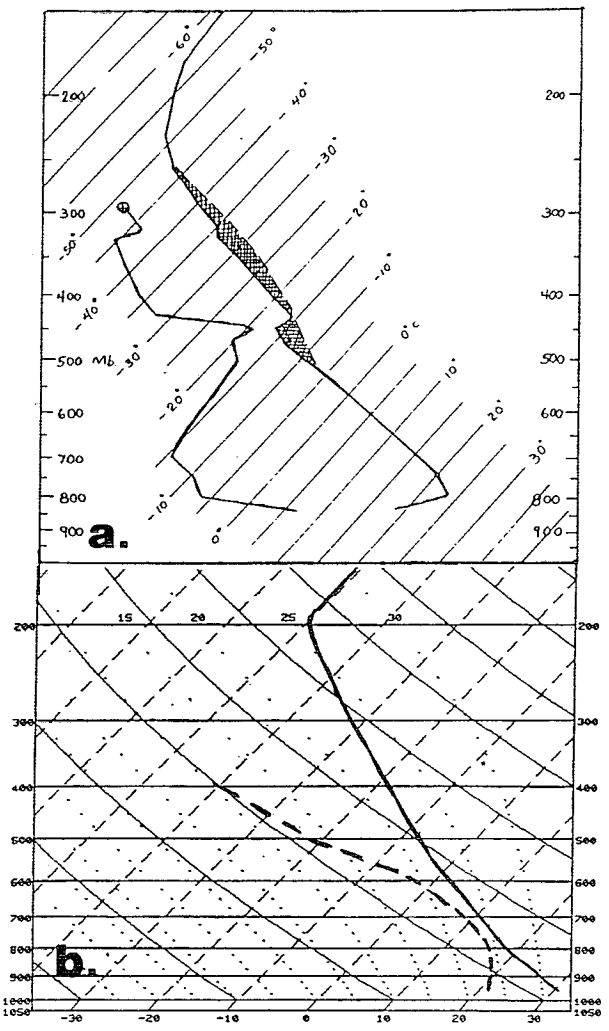

FIG. 6. (a) Skew T–log$p$ plot of the 1200 UTC 15 July 1982 Denver, Colorado, upper-air sounding (after Caracena et al. 1983). (b) Skew T–log$p$ conceptual model of sounding associated with wet downbursts in north Texas near onset (after Read 1987).

The wet microburst profile (Fig. 6b) typically displays high moisture values through a deep, surface-based layer, with the top of the moist layer sometimes extending beyond 4–5 km AGL. Relative humidities above the moist layer are typically low. As diurnal heating occurs, a dry-adiabatic layer can develop in the lower 1.5 km (5000 ft) AGL, so there may be weak to moderate potential instability and little or no capping inversion. Wet microbursts are also typically "pulse" in nature and occur during stagnant synoptic conditions.

A recent study by Atkins and Wakimoto (1991) suggests that the afternoon thermodynamic environment on active wet microburst days in a humid climate often displays a θ_e (equivalent potential temperature) *difference* between the surface and midlevels equal to or greater than 20°C (see Fig. 7). On thunderstorm days when no wet microburst activity was observed, θ_e differences were less than or equal to 13°C. This suggests that the vertical θ_e difference would be a potentially useful forecast parameter for strong wind gusts. Further, initial development of thunderstorms with microburst potential may be anticipated by determining where localized lifting is most likely, such as in the vicinity of topographic features and low-level boundaries (see Read 1987).

b. Wind gusts in moderate and strong shear environments

In situations where the vertical wind shear from the surface through midlevels is moderate or strong, convective wind forecasting becomes more complicated. In addition to the thermodynamic profile, the wind profile and the synoptic pattern also play a significant role in development of damaging winds. As vertical wind shear increases, deep convection is increasingly likely to take the form of self-perpetuating convective systems (i.e., the outflow systematically initiates new updrafts). These systems turn out to be responsible for most severe convective wind events. Figure 8 illustrates the range of self-perpetuating storm structures associated with damaging winds in moderate to strong wind-shear situations.

On the smaller end of the scale is the isolated supercell (Fig. 8a). Damaging outflow winds usually are associated with downdrafts accompanying such storms, but occasionally damaging *inflow* winds occur with su-

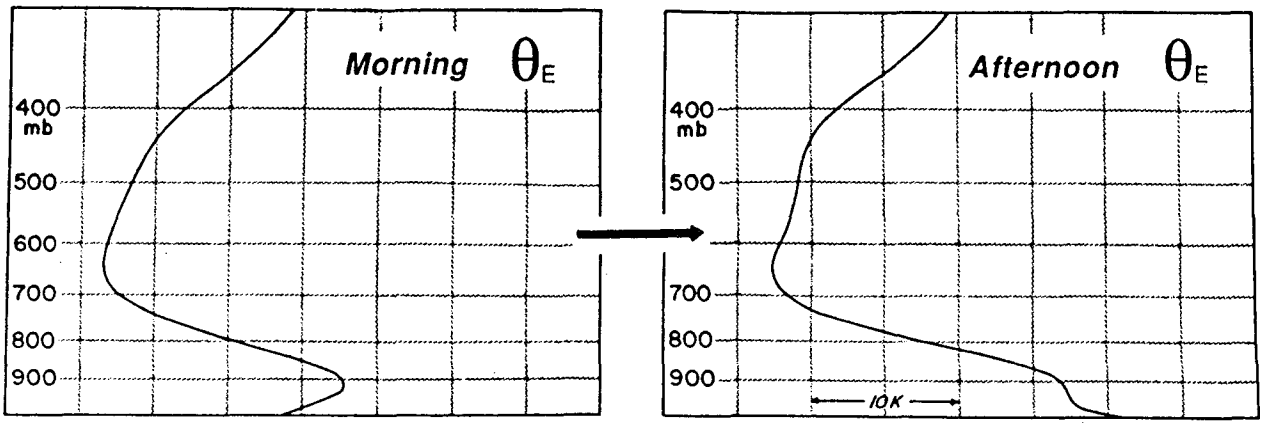

FIG. 7. Schematic θ_e profiles on days when the environment is conducive for wet microburst occurrence in a humid region (after Atkins and Wakimoto 1991).

percells. Typically, isolated supercells develop in a very unstable air mass exhibiting a capped "loaded gun" or "Type B" thermodynamic profile (Fig. 9) (Fawbush and Miller 1953; Barnes and Newton 1986), which is unstable for *both* updrafts and downdrafts. Winds usually veer strongly with height, resulting in the "crossing jets" pattern shown in Fig. 10a. Necessary ingredients for supercell development and forecasting of supercells will be discussed further in section 6.

A more common convective structure associated with damaging wind events occurring in moderate to strong wind-shear environments is the *bow echo* (Figs. 8b–d), as designated by Fujita (1978). Bow echoes are typically larger in scale than isolated supercells, and occasionally include embedded supercell circulations (e.g., Przybylinski and DeCaire 1985; Schmidt and Cotton 1989) that may produce tornadoes (e.g., Smith and Partacz 1985; Moller et al. 1990) as well as strong convective gusts. Bow-shaped echoes range in scale from less than 15 km (10 mi) to over 150 km (100 mi) in length, and often comprise components of an extensive convective line (see Fig. 8d). Some larger-scale bow echoes have smaller-scale bow echoes embedded within them. The curved bow-echo structure (Fig. 8b) apparently reflects the diverging outflow winds associated with a strong downdraft. Occasionally, a persistent large-scale bow echo or series of bow echoes produces a succession of downbursts that affect a widespread area (or swath). This larger-scale wind event has been called a *family of downburst clusters* (Fujita and Wakimoto 1981), or more recently, a *derecho* (Johns and Hirt 1987).

There are two basic synoptic patterns associated with bow-echo development: 1) the warm-season pattern, and 2) the dynamic pattern (Johns 1993). The warm-season pattern is most commonly observed during late spring and summer and is usually associated with progressive derechos (Fig. 11a). The convective activity develops in an area of low-level warm advection, along or north of a quasi-stationary boundary (Maddox and Doswell 1982; Johns 1984). An elevated rear-inflow jet (see, e.g., Augustine and Zipser 1987; Smull and

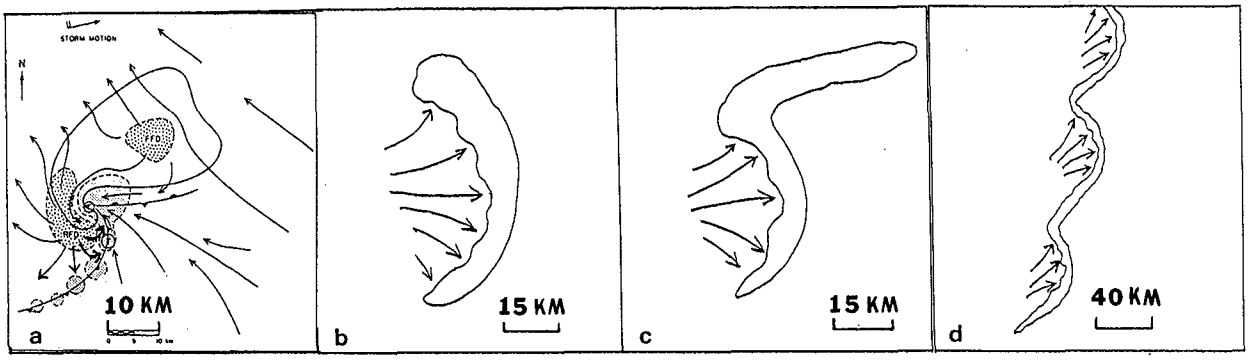

FIG. 8. (a) Schematic representation of flow associated with supercell thunderstorm (after Lemon and Doswell 1979), showing forward-flank downdraft (FFD), and rear-flank downdraft (RFD). (b) Schematic representation of downdraft flow associated with a relatively large bow echo. (c) As in (b) except for line-echo wave pattern form. Eastward extension from north end of bow echo is known as a warm advection wing (Smith 1990). (d) As in (b) except for extensive squall line with embedded bow echoes and line echo wave patterns.

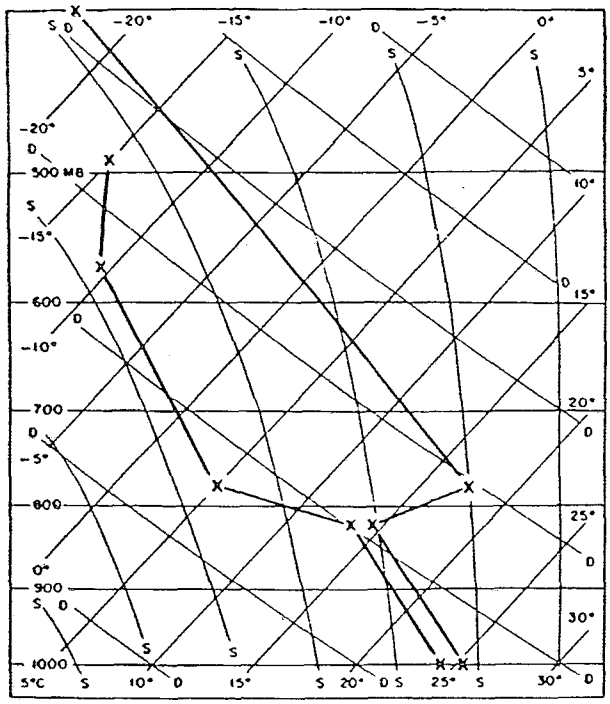

FIG. 9. Composite skew T–log$p$ plot of sounding (after Fawbush and Miller 1953) associated with tornadoes in the plains region, often referred to as the "loaded gun" or "Type B" sounding.

Houze 1987) is often found with these events, and it appears to be a critical factor in the initiation and maintenance of warm-season derechos (e.g., Burgess and Smull 1990; Schmidt et al. 1990).

Once formed, bow echoes move along the boundary, but usually slightly to the right of the mean flow. The air mass along the boundary in warm-season synoptic pattern cases is typically extremely unstable (Johns et al. 1990a), owing to high lapse rates in elevated mixed layers (see Lanicci and Warner 1991) and "pooling" of low-level moisture (i.e., development of an area or zone where dewpoints are higher than in the surrounding region) in the convergence zone near the boundary (Fig. 12). This strong instability (see, e.g., Fig. 9) appears to play a role in maintaining the elevated rear-inflow jet and the strong outflows near the surface gust front (Weisman 1990). The cap associated with the dry, high lapse-rate air in the lower midtroposphere plays a significant role in restricting southward development of bow-echo activity in the warm sector. Therefore, bow-echo structures in this type of pattern usually do not develop into extensive lines. Instead, they tend to take relatively short bow-echo or line-echo wave pattern (or LEWP; see Nolen 1959) forms (see Figs. 8b and 8c).

During the past few warm seasons, SELS forecasters have mentioned occasionally the possibility of progressive derecho development in the convective outlook when their composite prognoses indicate patterns and parameter values that favor such development. About once or twice a year, parameters known to favor warm-season progressive derecho development are quite strong and affect an extensive area. When a bow-echo complex develops in such a situation, SELS forecasters have the option of inserting "enhanced wording" into watches issued ahead of the bow-echo complex. Figure 13 shows an example of an enhanced wording watch issued during a particularly intense progressive derecho event.

The other basic synoptic pattern associated with bow-echo development is the dynamic pattern (Johns 1993). This pattern is usually associated with an extensive squall line that results in a serial derecho (Fig. 11b). It may occur at any time of year, but appears to

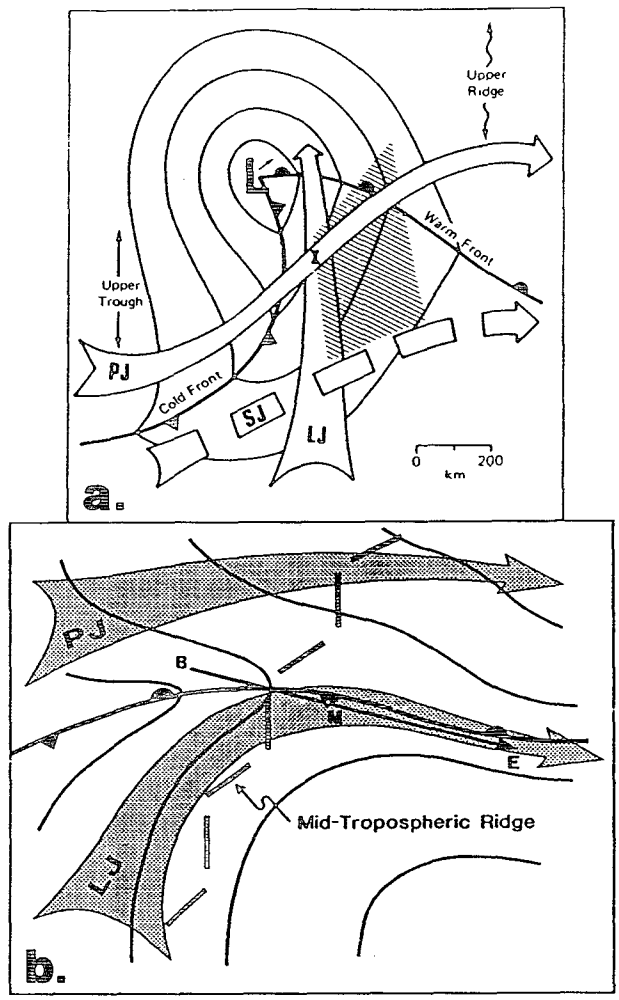

FIG. 10. (a) Idealized sketch (after Barnes and Newton 1986) of a middle-latitude synoptic-scale situation favorable for development of severe thunderstorms. Solid thin lines denote isobars, broad arrows represent low-level jet (LJ), polar jet (PJ), and subtropical jet (SJ). (b) As in (a), except for the situation associated with long-lived warm-season progressive derechos. The line denoted by B–M–E is the derecho's long axis, with B the beginning point (after Johns et al. 1990b).

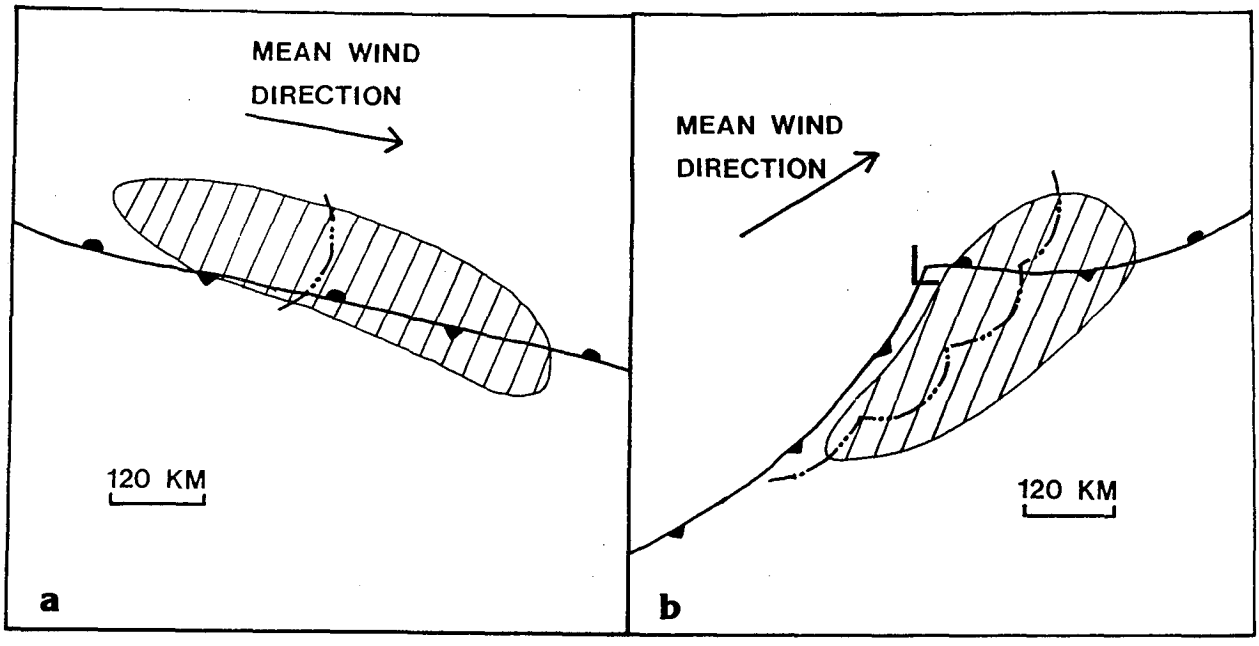

FIG. 11. (a) Schematic representation of features associated with a *progressive* derecho near midpoint of its lifetime. The total area affected by derecho during its lifetime is indicated by hatching; frontal and squall-line symbols are conventional. (b) As in (a), except for features associated with a *serial* derecho (after Johns and Hirt 1987).

be least common during mid- and late summer. It has some aspects of the classic severe weather outbreak (Forbes et al. 1980), usually involving a strong, progressive low pressure system (Fig. 10a). Since many cases occur during the cool season, however, the warm-sector air mass may be only marginally unstable and the vertical wind profile typically exhibits a pattern where upper- and low-level jets are more unidirectional than in the classic outbreak pattern (Johns 1993).

c. Climatology

Dry microbursts and inverted V soundings are most frequent on the High Plains and interior portions of

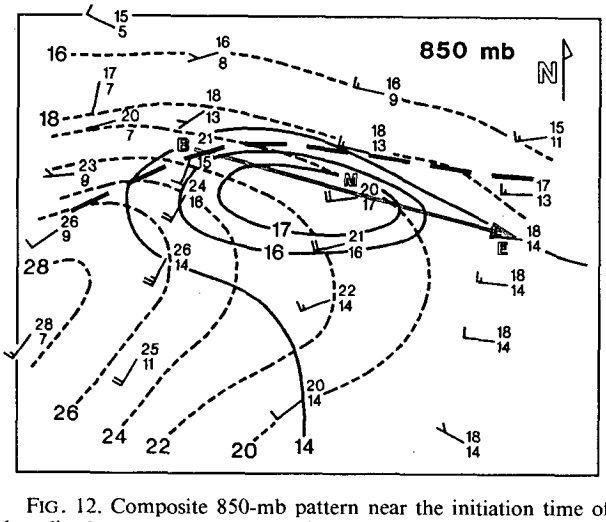

FIG. 12. Composite 850-mb pattern near the initiation time of long-lived warm-season progressive derechos (after Johns et al. 1990b). The solid arrow B–M–E is the derecho's long axis, with B its beginning point; the broad dashed line is a trough line (or 850-mb front); isotherms (dashed) and selected isodrosotherms (solid) are in °C. Full wind barbs equal 10 kt (5.1 m s^{-1}) and half-barbs equal 5 kt (2.6 m s^{-1}).

BULLETIN - IMMEDIATE BROADCAST REQUESTED
SEVERE THUNDERSTORM WATCH NUMBER 653
NATIONAL WEATHER SERVICE KANSAS CITY MO
1234 PM CDT SUN JUL 7 1991

.A..THE NATIONAL SEVERE STORMS FORECAST CENTER HAS ISSUED A SEVERE THUNDERSTORM WATCH FOR

MUCH OF CENTRAL AND SOUTHERN WISCONSIN
AND PORTIONS OF CENTRAL AND SOUTHERN LAKE MICHIGAN

FROM 130 PM UNTIL 800 PM CDT THIS SUNDAY AFTERNOON AND EVENING.

THIS IS A PARTICULARLY DANGEROUS SITUATION WITH THE POSSIBILITY OF EXTREMELY DAMAGING WINDS. LARGE HAIL AND DANGEROUS LIGHTNING ARE ALSO POSSIBLE.

THE SEVERE THUNDERSTORM WATCH AREA IS ALONG AND 70 STATUTE MILES EITHER SIDE OF A LINE FROM 30 MILES SOUTH OF LA CROSSE WISCONSIN TO 40 MILES NORTH NORTHEAST OF MILWAUKEE WISCONSIN.

REMEMBER...A SEVERE THUNDERSTORM WATCH MEANS CONDITIONS ARE FAVORABLE FOR SEVERE THUNDERSTORMS IN AND CLOSE TO THE WATCH AREA. PERSONS IN THESE AREAS SHOULD BE ON THE LOOKOUT FOR THREATENING WEATHER CONDITIONS AND LISTEN FOR LATER STATEMENTS AND POSSIBLE WARNINGS.

C... A FEW SVR TSTMS WITH HAIL SFC AND ALF TO 3 IN. EXTRM TURBC AND SFC WND GUSTS TO 90 KT. A FEW CBS WITH MAX TOPS TO 550. MEAN WIND VECTOR 27050.

D... DERECHO IN PROGRESS OVR NRN IA AND EXTRM SRN MN EXPCD TO CONT AS BOW ECHO SYS MOVS EWD ABT 50 KT ALG AND N OF QSTNRY BDRY. ISOLD WINDS OF 85 TO 90 KT PSBL.

E...OTR TSTMS... CONT VALID PTNS WW NR 649 THRU 652. WW MAY BE RQRD OVR PTNS NRN IL AND ERN IA IF TSTM LN DVLPS SWD DURG AFTN.

...JOHNS

FIG. 13. Example of a severe thunderstorm watch that contains "enhanced wording" for expected intense derecho winds. The watch was issued by the National Severe Storms Forecast Center during the long-lived derecho event of 7–8 July 1991.

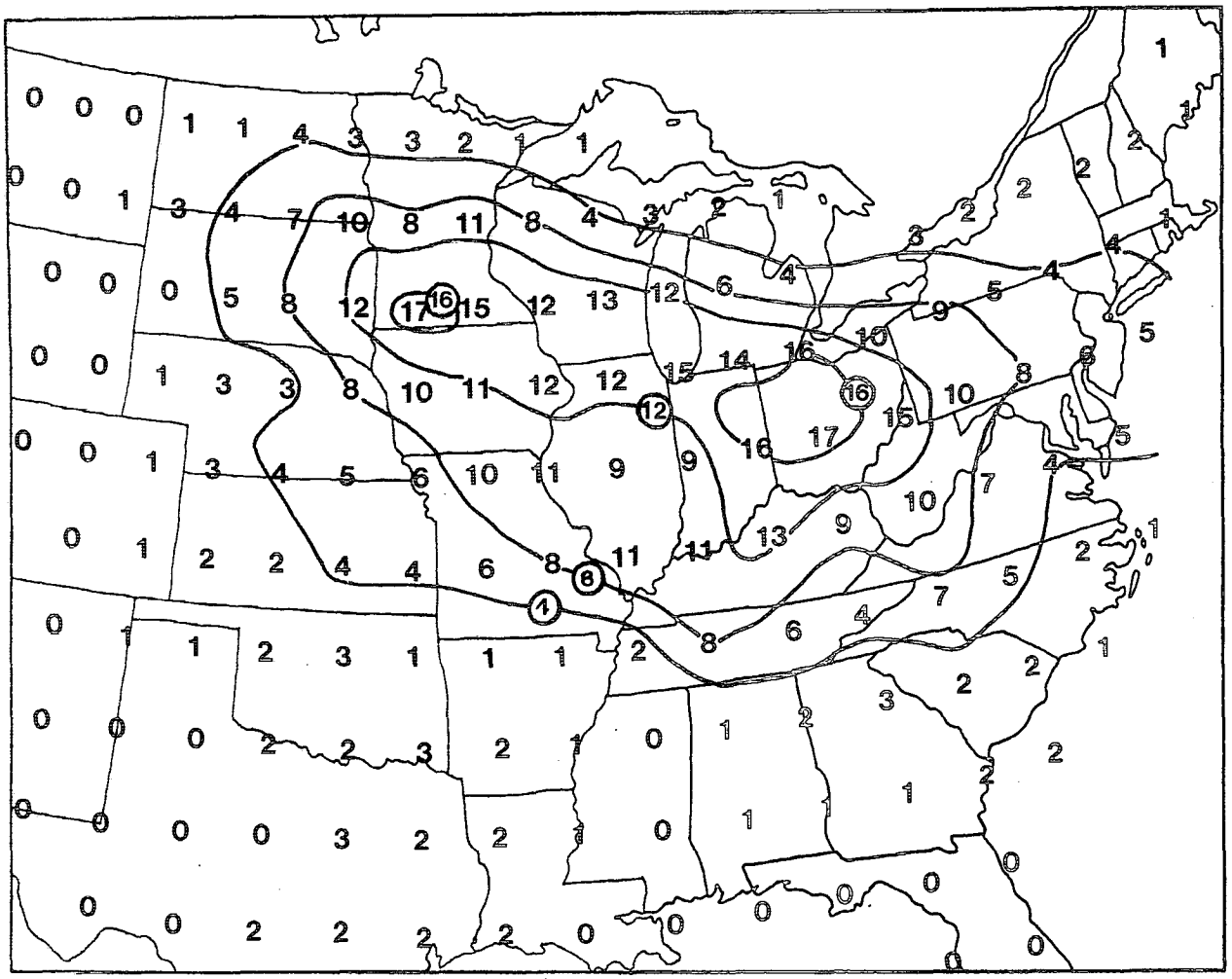

FIG. 14. Total number of derechos occurring in 2° latitude by 2° longitude squares during May through August for the period 1980–1983 (after Johns and Hirt 1987).

the west, while wet microbursts are most common east of the High Plains. Both types of pulse events are most common in summer and typically occur during the afternoon and early evening.

Isolated supercell and bow-echo wind events are most frequent in the afternoon and evening, but are less diurnally dependent than pulse storm microbursts. Isolated supercells are most likely in the plains during spring, while warm-season bow-echo events are most likely in late spring and summer in a band from the northern plains to the Ohio valley (Fig. 14). Operational experience suggests that dynamic synoptic pattern bow-echo events occurring during fall, winter, and early spring are most likely from the lower and mid–Mississippi valley eastward to the East Coast and are less diurnally dependent than other wind events.

6. Forecasting tornadoes

Tornadoes can be subdivided into two basic groups: those associated with supercells (e.g., Fig. 8a) and those that are not (e.g., as defined by Wakimoto and Wilson 1989).[4] *Nonsupercell tornadoes* are just beginning to be understood, and while some forecasting methods have been developed for them, such methods at present are tied to topographic features in specific locations. *Supercell tornadoes* include most of the strong and violent tornado events (F2 through F5, as classified by the F-scale system of Fujita 1971) and account for a disproportionate share of all tornado-related deaths, injuries, and damage. Owing to recent storm observations and numerical modeling experiments, much has been learned about supercell storms. The remainder of this section will primarily address the nature of supercell storm environments and current methods of forecasting supercell-induced tornado development.

[4] As with any classification scheme, we note that not every storm fits neatly into a category. See Doswell (1991b) for a discussion of classification schemes and their potential pitfalls.

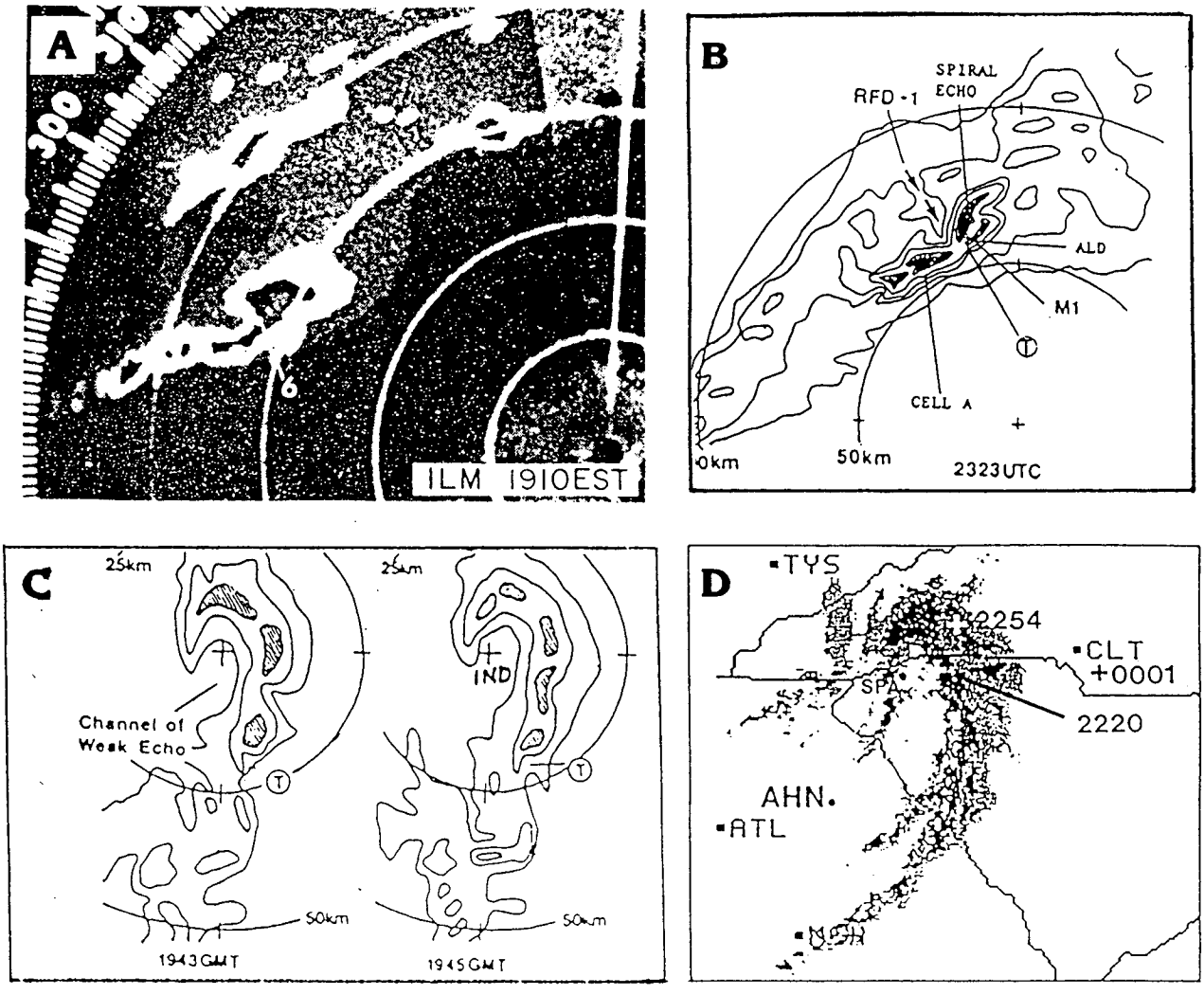

FIG. 15. Examples of complex convective structures (as indicated by radar reflectivity imagery) associated with strong and violent tornadoes: (a) F4 intensity McColl, South Carolina, tornado of 28 March 1984 (indicated by "6") associated with small bow echo (after *Storm Data* for March 1984); (b) F4 intensity Allendale, Illinois, tornado of 7 January 1989 (indicated by "T") associated with a short line (after Przybylinski et al. 1990); (c) F3 intensity Martinsville, Indiana, tornado of 10 March 1986 (indicated by "T") associated with bow echo and possible line-echo wave pattern (after Przybylinski 1988); and (d) F4 intensity Chesnee, South Carolina, tornado of 5 May 1989 (indicated by white "+" for 2220 UTC) associated with a spiral band. Additional F4 tornadoes occurred at 2254 and 0001 UTC as indicated (after July 1990).

a. Storm structures associated with supercell circulations[5]

It appears that deep, persistent mesocyclones that seem to be associated with supercell tornadoes can occur within a broad range of storm structures (Doswell et al. 1990; Doswell and Burgess 1993). Further, recent observational evidence suggests that "classic" isolated supercells (Fig. 8a) account for less than half of all strong and violent tornadoes occurring in the United States (Johns et al. 1993). It appears that a majority of such events are associated with a variety of complex storm structures (as seen on radar), including bow echoes, LEWPs, and spiral-banded echoes (e.g., Fig. 15), virtually all of which contain a deep, persistent mesocyclone, but which do not fit traditional models of supercells. The high-precipitation supercell category, described in Moller et al. (1990), has been developed, in part, to account for these complex structures within a spectrum of supercell storms (Doswell et al. 1990).

b. Wind environments associated with supercell development

Observations and, especially, numerical model simulations suggest that the most critical environmental

[5] Supercell circulation is used here as a general term to include all convective storms with deep, persistent mesocyclones, regardless of the echo morphology depicted by radar reflectivity data.

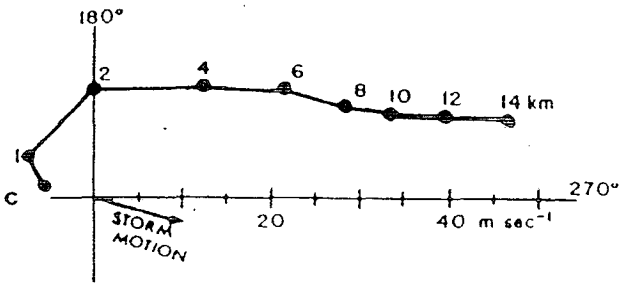

FIG. 16. Typical wind hodograph associated with supercell environments during the Alberta hail studies project (after Chisholm and Renick 1972).

factors affecting supercell development involve the strength and nature of tropospheric winds, particularly in the lower and middle layers. Numerical modeling experiments suggest that 1) the nature of the wind profile in the storm inflow layer (Weisman and Klemp 1984), 2) the strength of storm-relative inflow (Lazarus and Droegemeier 1990), and 3) the strength of wind shear through midlevels (Brooks et al. 1993) are all important for development and maintenance of supercell storms.

1) ROTATIONAL POTENTIAL OF THE STORM INFLOW LAYER

In an operational setting, it is difficult to define precisely what constitutes the storm inflow layer. Differing layers, generally within 4 km AGL, have been used to estimate the source of air entrained into the updraft (Browning and Landry 1963).[6] A study by Bluestein et al. (1989) suggests that, at least in very unstable "loaded gun" thermodynamic environments, entrainment into the updraft core is minimal above the LFC. Therefore, it is possible that in many cases the depth of the inflow layer is roughly coincident with LFC height (Davies and Johns 1993). Bluestein and Parks (1983) found that during spring, the average LFC height in supercell situations in the southern plains is slightly greater than 2 km AGL. In more moist and weakly capped situations (e.g., tropical cyclone environments) the LFC height may be significantly below 2 km AGL (e.g., McCaul 1991).

Streamwise vorticity (i.e., that part of the horizontal vorticity vector parallel to the flow) in the storm inflow layer results in updraft rotation when this air is ingested into an updraft (Davies-Jones 1984). The characteristic environment rich in streamwise vorticity has a hodograph that is strongly curved, with rapidly increasing speeds in the lower 2 or 3 km AGL (Fig. 16). Typically, hodographs associated with supercell development in the Northern Hemisphere (Southern Hemisphere) curve to the right (left). This requires veering of the *shear vector,* which produces the curved hodograph (see Doswell 1991a). Sometimes, supercells occur with relatively straight (only slightly curved) low-level hodographs when wind shear is sufficiently strong through a deep layer (e.g., Charba and Sasaki 1971). Therefore, the shape of the 0–3-km AGL segment of environmental hodographs associated with mesocyclone-induced tornadoes in the United States varies from only slightly to very strongly curved to the right (e.g., see Fig. 17).

Two parameters related to the inflow layer rotational potential are 1) *positive mean shear* (Davies 1989; Davies and Johns 1993) and 2) *storm-relative helicity* (Lilly 1986; Davies-Jones et al. 1990). Positive mean shear estimates the mean shear associated only with straight-line or right-turning segments of hodographs in the lowest 2 km AGL (approximating the inflow layer). Since this parameter evaluates the hodograph in a *ground-relative* framework, its applicability is affected by observed storm motions. Figure 18 illustrates the range of 0–2-km AGL positive shear values associated with a large dataset of 242 strong and violent tornadoes (occurring between April 1980 and March 1990) that was assimilated by Johns et al. (1990b, hereafter referred to as JDL).

Helicity, which is considered in a *storm-relative* framework, is a computationally more stable parameter than positive mean shear (Davies-Jones et al. 1990).

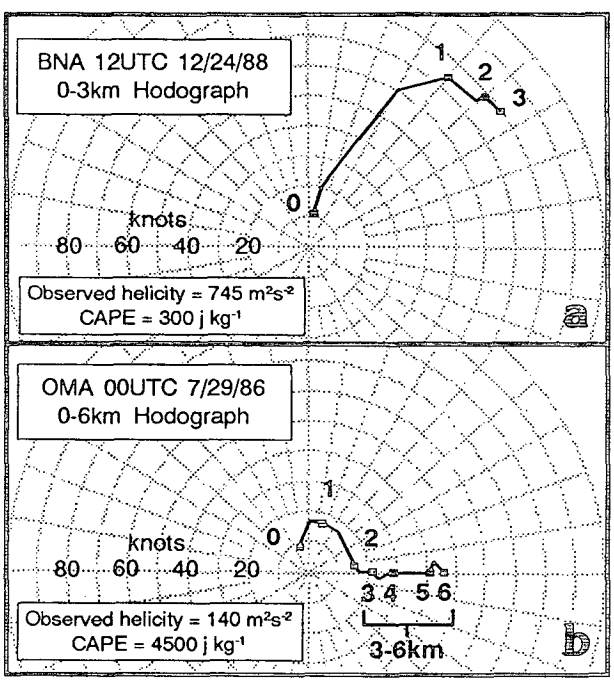

FIG. 17. Ground-relative hodographs (prepared by Jon Davies of Pratt, Kansas) for low-level wind structure (0–3 km AGL) at (a) Nashville, Tennessee, at 1200 UTC on 24 December 1988, and for low and midlevel wind structure (0–6 km AGL) at (b) Omaha, Nebraska, at 0000 UTC on 29 July 1986. The midlevel portion of the hodograph for Nashville was not available. Each ring increment represents 10 kt (5.1 m s^{-1}).

[6] In cases where convection is occurring above a frontal inversion, the inflow layer may have a base that is above the surface.

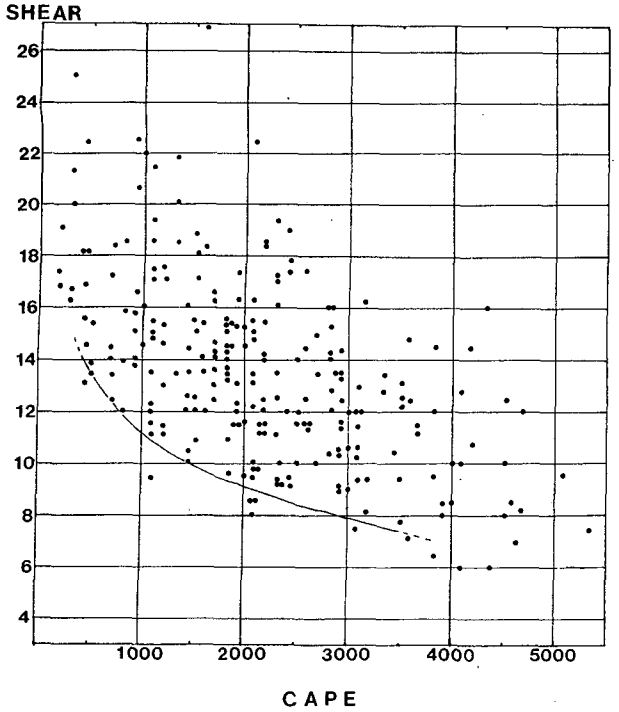

FIG. 18. Scatter diagram showing combinations of CAPE in J kg^{-1} and 0–2 km AGL positive wind shear ($\times 10^{-3}$ s^{-1}) for all 242 tornadoes in the JDL dataset. Solid curved line is a suggested lower limit of combined CAPE/low-level shear values that would support development of strong and violent tornadoes (after Johns et al. 1993).

Helicity can be visualized as twice the area swept out by the storm-relative motion vector in a layer (see Davies-Jones et al. 1990; Doswell 1991a). Therefore, the storm motion vector plays an important role in evaluating this parameter. Helicity values using *observed* storm motions have been calculated for limited data samples (Davies-Jones et al. 1990; Davies and Johns 1993), with results indicating that most strong and violent tornadoes in these datasets were associated with values in the 0–3-km layer greater than 300.

Forecasting storm motion can be a formidable task, since storm motions vary considerably from case to case (Davies and Johns 1993). Attempts have been made to assume an average storm motion based on the mean wind through deep layers of the troposphere [e.g., the cloud-bearing layer used by Maddox (1976) and the 0–6-km AGL layer used by Davies and Johns (1992)]. These "mean wind" methods for forecasting storm motion have met with limited success, at least in part because storm motions can be affected by other factors (e.g., Maddox et al. 1980; Johns et al. 1993) than the environmental flow.

Operational experience suggests that helicity (and low-level positive shear) values exhibit a diurnal oscillation, with a tendency for 1200 UTC values to be higher than those at 0000 UTC. This is particularly noticeable when dynamic forcing is weak, and appears to be related to the diurnal changes in the strength and nature of the low-level jet (e.g., Bonner 1968; Frisch et al. 1992). This diurnal low-level wind structure change directly affects helicity (Maddox 1993), which must be considered when forecasting updraft rotational potential.

Several forecasting methods involving parameters using wind forecasts by the operational NWP models have been developed or proposed (e.g., Woodall 1990; Davies and Johns 1993). Typically, these methods involve calculating helicity values from forecast winds for a variety of potential storm motions. A recently developed program at SELS displays hourly forecast hodographs and computes helicity values by using an assumed storm motion vector, the latest hourly surface wind, and NGM wind forecasts for selected points (see Fig. 5b). An experiment by Piltz (1992) suggests that hourly areal maps of helicity based on forecast (or observed) motions, surface data, and the lowest layers of wind profiler data (Dunn 1986) may become a helpful short-term forecast tool. These techniques have had limited evaluation, but appear to be most successful when the environmental winds are moderate to strong.

2) STRENGTH OF THE STORM INFLOW

A recent modeling study by Lazarus and Droegemeier (1990) suggests that storm-relative low-level inflow strength is a critical factor in the development of a strongly rotating updraft. Inflow strength is related to both storm motion and the strength and direction of winds in the inflow layer. One can estimate the potential environmental wind contribution to storm inflow by subtracting the mean tropospheric wind vector (which often is related to storm motion) from the mean wind vector in the storm inflow layer. The greater the resulting value is, the greater the range of storm motions that would result in sufficient inflow for strong rotation.

One also can determine the potential strength of storm-relative inflow in a particular situation by computing the difference between an estimated (e.g., Maddox 1976) or observed storm motion vector and the mean wind vector for the inflow layer. The SHARP program (discussed in section 3) calculates inflow vectors and storm-relative layer mean inflow values.

3) STRENGTH OF SHEAR THROUGH MIDTROPOSPHERE

Sufficient wind shear through midlevels can be important to supercell development for two reasons: 1) it *removes precipitation from updrafts* by enhancing storm-relative flow, and 2) interaction of this deeper shear with storm updrafts can induce *vertical perturbation pressure gradients* (Rotunno and Klemp 1982) that increase updraft strength. Further, wind strength (and shear) in the midlevels affects storm motion, thus indirectly affecting storm inflow strength (Brooks et al. 1993). Most 0–6-km AGL (84%) and almost all midlevel (3–6-km AGL) mean wind speeds (96%) in the

JDL dataset are greater than 15 m s^{-1} (30 kt), as noted by Davies and Johns (1993).

Most of the time when wind speeds in the midlevels appear to be too weak to support supercell development, 0–2-km AGL positive shear and helicity values are also weak. On some occasions, however, 1200 UTC soundings may indicate the presence of a low-level jet in an area where midlevel winds are weak. The accompanying hodographs display a "spike" signature (see Fig. 19) that can alert the forecaster that, while the low-level shear and helicity parameters are relatively strong, the wind environment may not be conducive to development of strong rotation. In contrast, note that even though the hodograph associated with the violent tornado of 28 July 1986 (Fig. 17b) results in a relatively low value of observed storm-relative helicity (and positive shear), the midlevel segment (3–6 km) displays increasing wind speeds with height.

c. *Instability associated with supercell development*

The JDL dataset (Fig. 18) suggests that supercells occur in environments with an extremely wide range of CAPE, varying from 200 to 5300 J kg^{-1}. An explanation for the distribution of CAPE values in Fig. 18 is related to the respective seasonal availability of both wind and instability environments favorable for mesocyclone development. During the cool months, wind environments favorable for mesocyclone development are common and widespread. However, instability sufficient for thunderstorm development is infrequent, and when it is present, values often are relatively low. The reverse is true for the warmest months, when moderate to high values of instability are often widespread, but wind environments supportive of mesocyclone development are infrequent. It is not surprising, then, that most cases in the JDL dataset exhibit intermediate values of both instability and favorable wind environment parameters (see Figs. 18 and 20, and Fig. 2 in Davies and Johns 1993), and occur in the transition season of spring, when the areal patterns of instability and favorable wind environments most frequently coincide.

Figures 18 and 20 also suggest that many supercells occur in both very low and very high instability environments, however, with high shear associated with the low instability cases and vice versa. This tendency has been recognized by Rasmussen and Wilhelmson (1983) and Turcotte and Vigneux (1987), among others, leading to a proposed association between storm type and the bulk Richardson number (BRN; see Weisman and Klemp 1984). In low instability/strong shear cases (BRN < 15, below the supercell thresholds proposed by Weisman and Klemp), mesocyclones usually are associated with complex convective structures (see Fig. 15), as noted by Johns et al. (1993). Some of the high instability/weak shear cases (BRN > 45, exceeding the supercell threshold proposed by Weisman and Klemp) are associated with bow echoes and isolated supercells that either are moving faster than the 0–6-km AGL mean wind (Smith 1990; Korotky et al. 1993), or are *extreme* right-moving supercells (Darkow and McCann 1977). In the former case, the environmental low-level flow is usually relatively light and, in the latter case, storms often move more directly into the low-level flow. In either case, storm-relative helicity and inflow often are enhanced by deviant cell movement.

d. *Supercells and tornadoes*

Forecasting supercells is *not* equivalent to forecasting tornadoes. For example, Doppler radar observations at the National Severe Storms Laboratory suggest that only about 50% (or perhaps less) of all Doppler-detected mesocyclones occurring in the southern plains in spring produce tornadoes (Burgess and Lemon 1990). One factor important for tornado generation is the strength of the outflow from storm downdrafts (see Fig. 8). Evaporatively cooled downdraft outflow results in a baroclinically generated, low-level contribution to vorticity that is critical for tornadogenesis (Rotunno and Klemp 1985; Davies-Jones and Brooks 1993). Some recent modeling results (Brooks et al. 1993) also suggest that if the outflow is *too* strong, it terminates tornadogenesis prematurely. The details of supercell tornadogenesis are not entirely resolved as yet, so the development of refined forecasting techniques must await further research. Generally, SELS forecasters consider that the presence of at least some "dry" (nonsaturated) air in the downdraft entrainment region is necessary for both bow echo–induced damaging winds (see subsection 5b) and supercell tornado development. Further, from the SELS perspective, the likelihood of supercell development (see subsections 6b and c) is the major factor in choosing between severe thunderstorm and tornado watches, except in cases (described next) where nonsupercell tornadoes can be anticipated reliably.

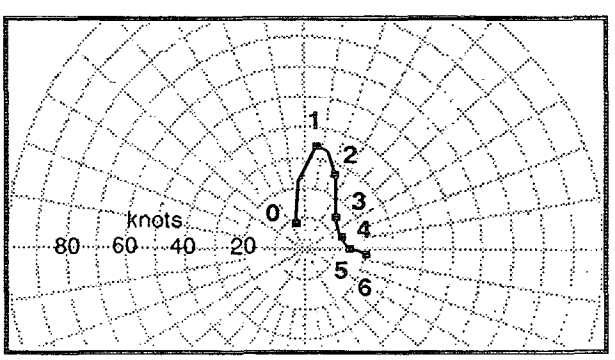

FIG. 19. Schematic representation of a ground-relative, 0–6-km AGL "spiked" hodograph (see text for definition) in which midlevel flow is usually insufficient for supercell development. Each ring increment represents 10 kt (5.1 m s^{-1}) (prepared by Jon Davies of Pratt, Kansas).

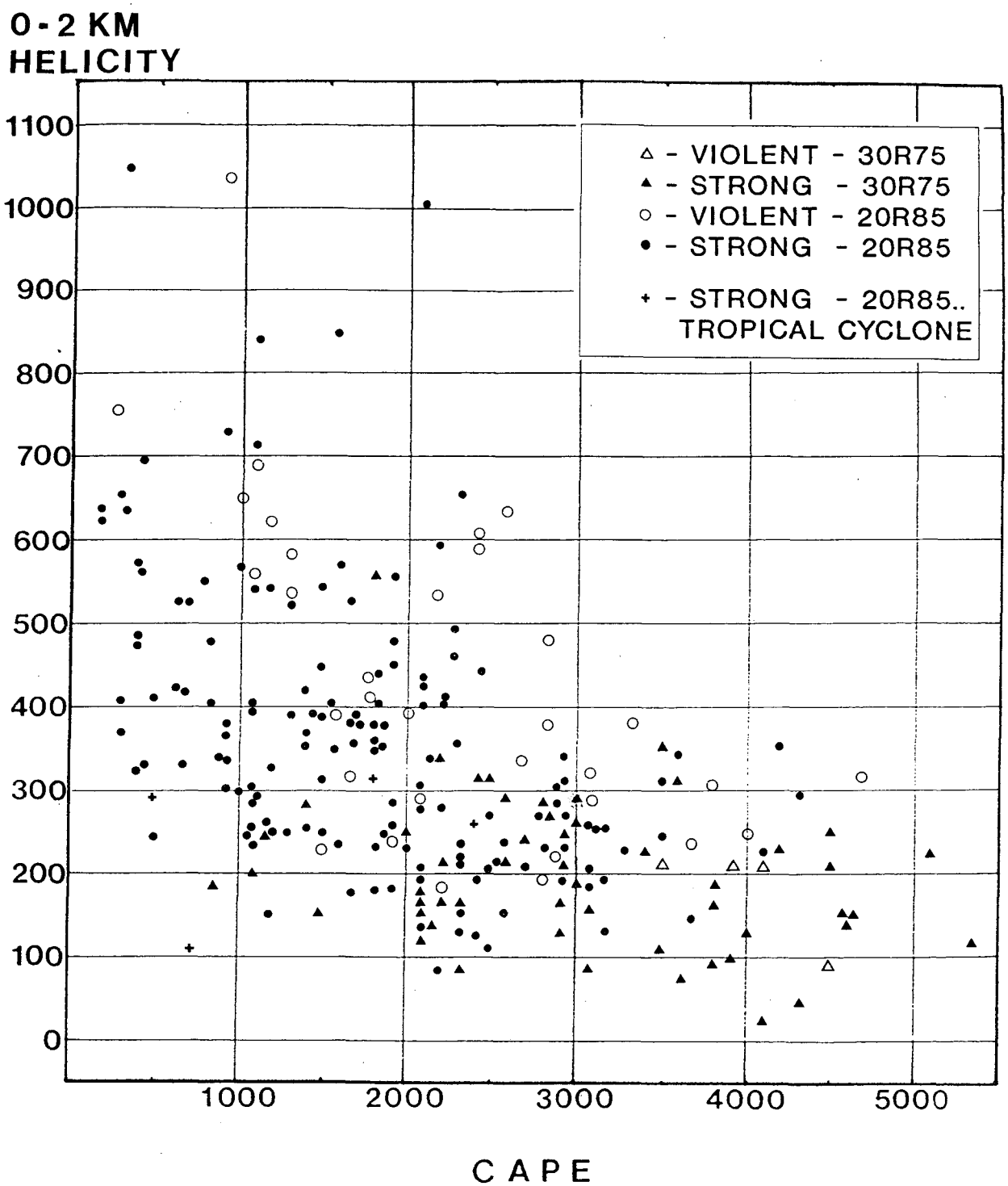

FIG. 20. Scatter diagram (after Johns et al. 1993) showing combinations of CAPE (J kg^{-1}) and 0–2-km AGL helicity (m^2 s^{-2}) utilizing the 20R85/30R75 storm motion assumptions for 242 strong and violent tornadoes of JDL dataset. All triangles (open and solid) represent cases in which the assumed storm motion is 30R75, while the assumed storm motion for the remainder of the cases is 20R85. The open circles and open triangles represent violent tornadoes (F4–F5). The crosses represent cases associated with tropical cyclones.

e. Pattern recognition

Pattern recognition continues to play an important role in tornado forecasting, and is particularly important for identifying potential outbreaks. The "classic" tornado outbreak exhibits a synoptic pattern similar to Miller's (1972) Type B (Fig. 10a) tornado pattern, and is characterized by an unusually strong, progressive extratropical cyclone. Typically, in such situations, an upper-level jet streak is associated with corresponding wind maxima at mid- and low levels, and a vertical wind profile favorable for supercell development results, as the mid- and low-level jet maxima come into proximity (Uccellini and Johnson 1979; Uccellini 1990). Tornado potential with this pattern is enhanced if the associated upper shortwave trough is moving rapidly, if it is negatively tilted, and/or if there is significant upper diffluence ahead of the trough. These empirical factors likely relate to developing a juxtaposition of synoptic-scale upward vertical motion and a steepening lapse rate (McNulty 1978), rapid influx of low-level moisture, and a supercell-favorable wind profile (i.e., winds are strong at all levels and veer strongly with height). When all of these factors are present, the result is what Doswell et al. (1993) call a "synoptically evident" or "big" tornado day (in the United States there are about 10 such days per year). When the SELS forecaster's composite prognoses indicate that all ingredients for a "big" day are likely to become coincident, the potential for a major tornado outbreak is highlighted in the SELS convective outlooks and a "public severe weather outlook" stressing the threat is issued. If short-term indicators continue to be favorable as the day in question progresses, enhanced wording that emphasizes the outbreak potential is included in tornado watches for the affected area (see Fig. 5 in Doswell et al. 1993 for an example).

Most other tornado episodes tend to be more localized than the "big" days, but still may include strong or violent tornadoes. These can occur with a variety of synoptic patterns. Many exhibit some variation of the "synoptically evident" outbreak patterns. Typically, in such cases, either 1) the necessary parameters are in juxtaposition but one (or more) of the parameters is marginal for tornado development (e.g., the wind maximum in the low-level jet may be only marginally strong), or 2) all of the necessary parameters are strong, but are not in juxtaposition (e.g., the maximum in the low-level jet may not be in close proximity to the maximum in the midlevel jet).

Also, some synoptic patterns associated with localized tornadic episodes differ considerably from the "synoptically evident" patterns. Two such atypical patterns are Miller's (1972) "warm advection pattern" (Type C) and "cold low/occluded front pattern" (Type D). In the warm advection pattern, tornado activity occurs near a quasi-stationary or warm frontal boundary oriented roughly parallel to the midlevel flow. The associated shortwave trough is usually weak to moderate in intensity. Operational experience suggests that from late winter into early spring, this pattern is most often associated with a westerly subtropical jet stream across the Gulf Coast states (e.g., Branick 1981). From late spring into summer, this pattern is commonly associated with "northwest flow" outbreaks (e.g., Johns and Leftwich 1988; LaPenta et al. 1990).

The cold low/occluded front tornado pattern (Type D) is associated with a cold upper low and/or an occluded front that is in proximity to a cold upper low. Given sufficient instability, tornadoes may occur with thunderstorms developing near the upper low (Cooley 1978; Goetsch 1988). These events develop from relatively low-topped convection that is usually nonsupercellular in nature. Tornadoes also may occur along the occluded front toward the warm sector (e.g., Carr and Millard 1985; Moore and Elkins 1985). Typically, the wind profile becomes more favorable for supercells away from the upper low and toward the midlevel jet.

A localized, topography-dependent tornado pattern is the "Los Angeles basin pattern" (Hales 1985). When a deep, occluded low develops off the central/southern California coast, the coastline shape and inland terrain promote development of a favorable low-level wind profile for supercell development in the Los Angeles basin. There are likely other areas in the United States where specific synoptic patterns and local topography combine to induce favorable wind profiles for supercells (e.g., see Braun and Monteverdi 1991).

Nonsupercell tornadoes also may be favored by unique terrain and wind patterns. For example, Szoke and Augustine (1990) have described the "Denver cyclone" pattern, which often includes tornado events. The Denver cyclone is a mesoscale surface low pressure center (or zone) and an associated low-level convergence boundary zone that develops near Denver, Colorado, prior to convection in certain synoptic-flow regimes. Such phenomena may be found in other places as well, but if so, they are not documented.

Thermodynamic and wind profiles can display common patterns for a particular type of tornado situation. For example, tornado outbreaks occurring in the central and southern Great Plains in spring are typically associated with a "loaded gun" thermodynamic profile (Fig. 9) and a hodograph that curves markedly to the right in the first 2 or 3 km AGL, while being generally straight with increasing wind speeds above 3 km AGL (e.g., Fig. 16). On the other hand, thermodynamic and wind profile patterns associated with tropical cyclone tornadoes (Fig. 21) are strikingly different from those associated with both Great Plains springtime tornado outbreaks and Oklahoma supercells (McCaul 1991). The composite hodograph in tropical cyclone cases displays a very large loop that approaches being a circle. This wind profile appears to be highly supportive of supercell development but the composite thermodynamic profile displays relatively moist air

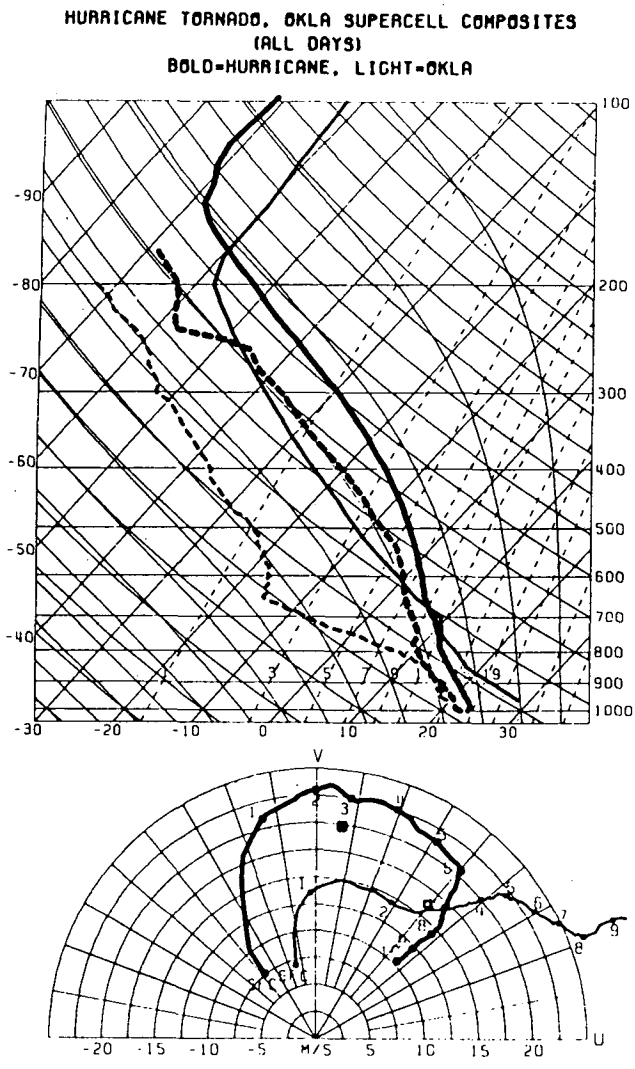

FIG. 21. Skew T–log$p$ plots and hodograph diagrams (after McCaul 1991) for the tropical cyclone close-proximity composite (heavy line) and Oklahoma supercell composite of Bluestein and Jain (1985) (light line). The u and v components of the Oklahoma composite are relative to true zonal and meridional directions; boxes indicate 0–6-km AGL mean winds.

through midlevels and has relatively little CAPE. In such situations, primary forecast problems often are whether instability will be sufficient for deep convection to develop and whether there will be sufficient dry air in the downdraft entrainment layer to support development of downdrafts and associated low-level baroclinic vorticity for tornadogenesis.

f. Climatology

Several aspects of tornado climatology can alert the forecaster to those times and areas where he/she must have increased awareness of the potential tornado threat. For example, tornado outbreaks (10 or more events) occurring in winter are most likely from the Gulf coastal states into the mid–Mississippi valley (Galway 1977; Galway and Pearson 1981). In Florida during the winter and early spring, most tornadoes of strong or violent intensity occur between midnight and noon LST (Fig. 22). Further, Maddox (1993) has shown that most F3 or greater intensity United States tornadoes that are reported between 0600 and 1200 UTC (0000 and 0600 CST) occur in the Gulf Coast states. Tornadoes occurring in the western United States coastal regions are most common from fall through early spring (McNulty 1981). Tornadoes associated with tropical cyclones affecting the United States are most likely in late summer and early fall and most typically occur with those cyclones that move inland from the Gulf of Mexico or that portion of the Atlantic coastline south of 32° latitude (Weiss 1987b). It is accepted generally that Northern Hemisphere tornadoes occur most typically with southwesterly flow aloft in the warm sector (see Fig. 10a); however, synoptic climatologies indicate that northwesterly flow in the warm sector often is associated with tornadoes that occur in late spring and summer from the upper Mississippi valley to the Mid-Atlantic states (Johns 1982; Giordano and Fritsch 1991).

These are some examples of where regional tornado climatology indicates a significant variation from the overall climatology (e.g., Kelly et al. 1978). This information allows a forecaster in a particular region to adjust his/her climatological expectations accordingly.

7. Discussion

Knowledge of the processes and parameters associated with severe local storms has advanced rapidly in recent years. These advances have resulted primarily from a combination of numerical model simulation experiments and observational studies. This increased understanding has led to several new forecast techniques that are aiding SELS forecasters in assessing the

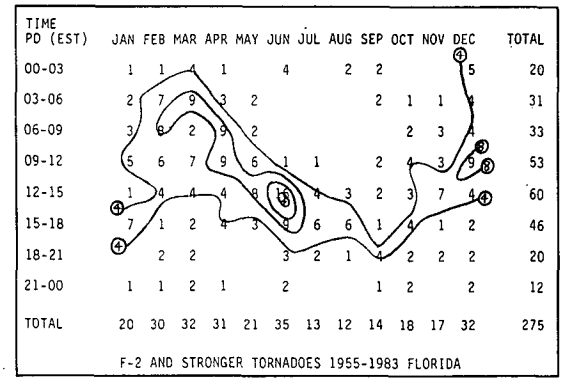

FIG. 22. Diurnal and seasonal frequency for all (275) strong and violent Florida tornadoes occurring from 1955 through 1983 (from the NSSFC database). Numbers in the grid represent cases occurring during a particular 3-h period of the day for each month.

potential for severe local storm development. This is particularly true for supercell tornadoes, "pulse" storm microbursts, and bow-echo damaging winds.

New observational technology is aiding SELS forecasters in the "diagnosis and trend" aspect of assessing severe local storm potential. New datasets include cloud-to-ground lightning strikes, aircraft-measured winds, WSR-88D radar imagery, wind profilers, and so on. An increased density (in populous areas) of surface data from automated stations is currently available for some areas of the United States, and these new data sources are expected to become national in scope within the next few years. Regional *mesoscale* networks of surface stations (e.g., Crawford et al. 1992) also may become available in the near future. All these new data sources are helping remove broad temporal and spatial gaps in the operational data network. Because subsynoptic-scale analysis has been hampered by lack of adequate operational data, SELS forecasters have found immediate utility in these new data sources even though national coverage is incomplete and some sources are "experimental" (e.g., see Fig. 1a).

Another development in the last few years that has aided in the assessment of severe local storm potential is access to the full range of numerical model outputs, allowing development of model forecast fields that are relevant to the severe local storm forecast problem (e.g., sounding and hodograph forecasts). Further, development of more powerful computers (and software) is allowing more comprehensive diagnosis of the forecast data, thereby making the output more useful.

The new forecast techniques require that the forecaster examine existing and model forecast conditions in more detail, while the new observational data sources and model products provide massive amounts of data for the forecaster to sort through. Given the time constraints of forecasting, operational meteorologists are increasingly feeling as if they are "drowning in a sea of data." The keys are to focus on those data that are relevant to the situation, and to display them in a useful manner. Development of procedures to do this is an ongoing process that continues as new interpretation techniques and data sources come into operational practice.

Our changing perceptions of the complex processes associated with development of severe local storms make the utility of fixed meteorological checklists (e.g., Colquhoun 1987) problematic. However, some form of a data-management checklist or priority list may become a necessity if the forecaster is to effectively use all the new interpretation techniques and data sources to arrive at more accurate and timely forecasts.

If the data management and interpretation challenges can be met, some continued improvement of the parameter assessment and pattern recognition aspects of forecasting is likely. Such improvements, however, will depend on the ability to achieve an accurate current analysis of meteorological conditions and the ability of operational NWP models to forecast changes in critical severe weather parameters accurately. One can be hopeful that new observational technologies that are being implemented operationally (e.g., WSR-88D Doppler radars), are undergoing experimental evaluation (wind profilers), or are likely to be evaluated in the near future (thermal and moisture profilers) will help to fill the temporal and spatial data gaps. Also, experiments by numerical modelers should lead to operational synoptic- and mesoscale model forecasts that have greater accuracy in predicting severe weather parameters. The pattern recognition and climatological aspects of severe weather forecasting likely will continue to be important to the forecasting process in the future, however, since they help alert the forecaster to when and where he/she should concentrate more closely on the potential for severe weather development.

Acknowledgments. The authors especially appreciate the numerous beneficial suggestions offered by Steve Weiss of NSSFC. Fred Ostby, Jim Henderson, John Hart, and Bill Sammler (all of NSSFC), Josh Korotky (OSF Training Branch), Harold Brooks (NSSL), Steve Lyons (NWS Southern Region Headquarters), Jon Davies, and the anonymous reviewers also made many constructive suggestions. The authors are grateful for the assistance of Phillip Bothwell, Alan Cope, Jon Davies, and Ron Przybylinski in preparing the figures, as well as to Deborah Haynes and Kevin McCarthy for helping with manuscript preparation.

REFERENCES

Anthes, R. A., 1977: A cumulus parameterization scheme utilizing a one-dimensional cloud model. *Mon. Wea. Rev.*, **105**, 270–286.

Anthony, R. W., 1988: Tornado/severe thunderstorm climatology for the southeastern United States. Preprints, *15th Conf. Severe Local Storms*, Baltimore, Amer. Meteor. Soc., 511–516.

Atkins, N. T., and R. M. Wakimoto, 1991: Wet microburst activity over the southeastern United States: Implications for forecasting. *Wea. Forecasting*, **6**, 470–482.

Augustine, J. A., and E. J. Zipser, 1987: The use of wind profilers in a mesoscale experiment. *Bull. Amer. Meteor. Soc.*, **68**, 4–17.

Barnes, S. L., and C. W. Newton, 1986: Thunderstorms in the synoptic setting. *Thunderstorms: A Social, Scientific, and Technological Documentary. Vol. 2: Thunderstorm Morphology and Dynamics*, 2nd edition, E. Kessler, Ed., University of Oklahoma Press, 75–111.

Beebe, R. G., 1955: Types of airmasses in which tornadoes occur. *Bull. Amer. Meteor. Soc.*, **36**, 349–350.

Bluestein, H. B., and C. R. Parks, 1983: A synoptic and photographic climatology of low-precipitation severe thunderstorms in the Southern Plains. *Mon. Wea. Rev.*, **111**, 2034–2046.

——, and M. H. Jain, 1985: Formation of mesoscale lines of precipitation: Severe squall lines in Oklahoma during the spring. *J. Atmos. Sci.*, **42**, 1711–1732.

——, E. W. McCaul, Jr., G. P. Byrd, and G. R. Woodall, 1989: Mobile sounding observations of a tornadic thunderstorm near the dryline: The Gruver, Texas, storm complex of 25 May 1987. *Mon. Wea. Rev.*, **117**, 244–250.

Bonner, W. D., 1968: Climatology of the low-level jet. *Mon. Wea. Rev.*, **96**, 833–850.

Bothwell, P. D., 1992: An interactive skew-*T* program for combining observed and model data. Preprints, *8th Int. Conf. on Interactive Information and Processing Systems for Meteor., Oceanogr., and Hydrol.*, Atlanta, Amer. Meteor. Soc., 135–140.

Brandes, E. A., 1977: Gust front evolution and tornado genesis as viewed by Doppler radar. *J. Appl. Meteor.*, **16,** 333–338.

Branick, M. L., 1981: Meteorological analysis of a severe supercell thunderstorm over southern Mississippi, 31 March 1981. Southern Topics, July 1981, Southern Region Headquarters NWS, Ft. Worth, Texas, 7 pp.

Braun, S. A., and J. P. Monteverdi, 1991: An analysis of a mesocyclone-induced tornado occurrence in northern California. *Wea. Forecasting,* **6,** 13–31.

Brooks, H. E., and R. B. Wilhelmson, 1990: The effects of low-level hodograph curvature on supercell structure. Preprints, *16th Conf. Severe Local Storms,* Kananaskis Park, Alberta, Canada, Amer. Meteor. Soc., 34–39.

——, C. A. Doswell III, and R. P. Davies-Jones, 1993: Environmental helicity and the maintenance and evolution of low-level mesocyclones. *Proc., Tornado Symp. III,* C. Church, Ed., Amer. Geophys. Union, (in press).

Browning, K. A., and C. R. Landry, 1963: Airflow within a tornadic storm. Preprints, *10th Wea. Radar Conf.,* Washington, D.C., Amer. Meteor. Soc., 116–122.

Browning, P. A., 1991: The VDUC Interactive Computer System at the National Severe Storms Forecast Center. *Proc., Seventh Int. Conf. on Interactive Information and Processing Systems for Meteor., Oceanogr., and Hydrol.,* New Orleans, Amer. Meteor. Soc., 204–207.

——, 1992: Use of interactive workstations in the NSSFC forecast operations. Preprints, *Eighth International Conf. Interactive Info. and Processing Systems for Meteor., Oceanogr., and Hydrol.,* Atlanta, Amer. Meteor. Soc., 233–237.

Burgess, D. W., and P. S. Ray, 1986: Principles of radar. *Mesoscale Meteorology and Forecasting,* P. S. Ray, Ed., Amer. Meteor. Soc., 85–117.

——, and L. R. Lemon, 1990: Severe thunderstorm detection by radar. *Radar in Meteorology,* D. Atlas, Ed., Amer. Meteor. Soc., 619–647.

——, and B. F. Smull, 1990: Doppler radar observations of a bow echo associated with a long-track severe windstorm. Preprints, *16th Conf. Severe Local Storms,* Kananaskis Park, Alberta, Canada, Amer. Meteor. Soc., 203–208.

Caracena, F., J. McCarthy, and J. A. Flueck, 1983: Forecasting the likelihood of microbursts along the front range of Colorado. Preprints, *13th Conf. Severe Local Storms,* Tulsa, Oklahoma, Amer. Meteor. Soc., 261–264.

Carr, F. H., and J. P. Millard, 1985: A composite study of comma clouds and the association with severe weather over the Great Plains. *Mon. Wea. Rev.,* **113,** 370–387.

Charba, J., and Y. Sasaki, 1971: Structure and movement of the severe thunderstorms of 3 April 1964 as revealed from radar and surface mesonetwork data analysis. *J. Meteor. Soc. Japan,* **49,** 191–213.

Chisholm, A. J., and J. H. Renick, 1972: The kinematics of multicell and supercell Alberta hailstorms. Alberta Hail Studies—1972, Research Council of Alberta Hail Studies, Rep. 72-2, Edmonton, Canada, 24–31.

Colquhoun, J. R., 1987: A decision tree method of forecasting thunderstorms, severe thunderstorms and tornadoes. *Wea. Forecasting,* **2,** 337–345.

Cooley, J. R., 1978: Cold air funnel clouds. *Mon. Wea. Rev.,* **106,** 1368–1372.

Cope, A. M., 1992: Visualization of numerical model output at the National Severe Storms Forecast Center. Preprints, *8th International Conf. Interactive Info. and Processing Systems for Meteor., Oceanogr., and Hydrol.,* Atlanta, Amer. Meteor. Soc., 141–144.

Crawford, C. C., F. V. Brock, R. L. Elliot, G. W. Cuperus, S. J. Stadler, H. L. Johnson, and C. A. Doswell III, 1992: The Oklahoma mesonetwork—A 21st century project. Preprints, *Eighth International Conf. Interactive Info. and Processing Systems for Meteor., Oceanogr., and Hydrol.,* Atlanta, Amer. Meteor. Soc., 27–33.

Darkow, G. L., and D. W. McCann, 1977: Relative environmental winds for 121 tornado bearing storms. Preprints, *11th Conf. Severe Local Storms,* Omaha, Nebraska, Amer. Meteor. Soc., 413–417.

Davies, J. M., 1989: On the use of shear magnitudes and hodographs in tornado forecasting. Preprints, *12th Conf. Wea. Analysis and Forecasting,* Monterey, California, Amer. Meteor. Soc., 219–224.

——, and R. H. Johns, 1993: Some wind and instability parameters associated with strong and violent tornadoes. Part I: Wind shear and helicity. *Proc., Tornado Symposium III,* C. Church, Ed., Amer. Geophys. Union, (in press).

Davies-Jones, R. P., 1984: Streamwise vorticity: The origin of updraft rotation in supercell storms. *J. Atmos. Sci.,* **41,** 2991–3006.

——, and H. Brooks, 1993: Mesocyclogenesis from a theoretical perspective. *Proc., Tornado Symp. III,* C. Church, Ed., Amer. Geophys. Union, (in press).

——, D. Burgess, and M. Foster, 1990: Test of helicity as a tornado forecast parameter. Preprints, *16th Conf. Severe Local Storms,* Kananaskis Park, Alberta, Canada, Amer. Meteor. Soc., 588–592.

Doswell, C. A. III, 1980: Synoptic-scale environments associated with High Plains severe thunderstorms. *Bull. Amer. Meteor. Soc.,* **61,** 1388–1400.

——, 1982: The operational meteorology of convective weather. Vol. I: Operational Mesoanalysis. NOAA Tech. Memo NWS NSSFC-5, 158 pp.

——, 1986a: The human element in weather forecasting. *Natl. Wea. Dig.,* **11,** 2, 6–17.

——, 1986b: Short-range forecasting. *Mesoscale Meteorology and Forecasting,* P. S. Ray, Ed., Amer. Meteor. Soc., 689–719.

——, 1987: The distinction between large-scale and mesoscale contribution to severe convection: A case study example. *Wea. Forecasting,* **2,** 3–16.

——, 1991a: A review for forecasters on the applications of hodographs to forecasting severe thunderstorms. *Natl. Wea. Dig.,* **16,** 1, 2–16.

——, 1991b: Comments on "Mesoscale convective patterns of the southern High Plains." *Bull. Amer. Meteor. Soc.,* **72,** 389–390.

——, and D. W. Burgess, 1993: Tornadoes and tornadic storms: A review of conceptual models. *Proc., Tornado Symp. III,* C. Church, Ed., Amer. Geophys. Union, (in press).

——, J. T. Schaefer, D. W. McCann, T. W. Schlatter, and H. B. Wobus, 1982: Thermodynamic analysis procedures at the National Severe Storms Forecast Center. Preprints, *Ninth Conf. Wea. Forecasting and Analysis,* Seattle, Amer. Meteor. Soc., 304–309.

——, A. R. Moller, and R. Przybylinski, 1990: A unified set of conceptual models for variations on the supercell theme. Preprints, *16th Conf. Severe Local Storms,* Kananaskis Park, Alberta, Canada, Amer. Meteor. Soc., 40–45.

——, S. J. Weiss, and R. H. Johns, 1993: Tornado forecasting—a review. *Proc., Tornado Symp. III,* C. Church, Ed., Amer. Geophys. Union, (in press).

Dunn, L., 1986: An example of subjective interpretation of network profiler data in real-time forecasting. *Wea. Forecasting,* **1,** 219–225.

Fawbush, E. J., and R. C. Miller, 1953: A method for forecasting hailstone size at the earth's surface. *Bull. Amer. Meteor. Soc.,* **34,** 235–244.

——, and ——, 1954: A basis for forecasting peak wind gusts in nonfrontal thunderstorms. *Bull. Amer. Meteor. Soc.,* **35,** 14–19.

Forbes, G. S., M. J. Markus, and G. D. Lessens, 1980: Some synoptic and mesoscale factors associated with downburst-producing thunderstorms. Preprints, *Eighth Conf. Wea. Forecasting and Analysis,* Denver, Amer. Meteor. Soc., 363–369.

Foster, D. S., 1958: Thunderstorm gusts compared with computed downdraft speeds. *Mon. Wea. Rev.,* **86,** 91–94.

——, and F. Bates, 1956: A hail size forecasting technique. *Bull. Amer. Meteor. Soc.,* **37,** 135–140.

Frisch, A. S., B. W. Orr, and B. E. Martner, 1992: Doppler radar observations of the development of a boundary-layer nocturnal jet. *Mon. Wea. Rev.,* **120,** 3–16.

Fujita, T. T., 1971: Proposed characterization of tornadoes and hur-

ricanes by area and intensity. SMRP Res. Pap. No. 91, Dept. of Geophysical Sciences, University of Chicago, 42 pp.
——, 1978: Manual of downburst identification for project NIMROD. Satellite and Mesometeorology Res. Pap. No. 156, University of Chicago, Dept. of Geophysical Sciences, 104 pp.
——, and H. R. Byers, 1977: Spearhead echo and downburst in the crash of an airliner. *Mon. Wea. Rev.*, **105,** 129–146.
——, and R. M. Wakimoto, 1981: Five scales of airflow associated with a series of downbursts on 16 July 1980. *Mon. Wea. Rev.*, **109,** 1438–1456.
Galway, J. G., 1956: The lifted index as a predictor of latent instability. *Bull. Amer. Meteor. Soc.*, **37,** 528–529.
——, 1977: Some climatological aspects of tornado outbreaks. *Mon. Wea. Rev.*, **105,** 477–484.
——, and A. Pearson, 1981: Winter tornado outbreaks. *Mon. Wea. Rev.*, **109,** 1072–1080.
Giordano, L. A., and J. M. Fritsch, 1991: Strong tornadoes and flash-flood producing rainstorms during the warm season in the Mid-Atlantic region. *Wea. Forecasting,* **6,** 437–455.
Goetsch, E. H., 1988: Forecasting cold core severe weather outbreaks. Preprints, *15th Conf. Severe Local Storms,* Baltimore, Amer. Meteor. Soc., 468–471.
Hales, J. E., Jr., 1979: A subjective assessment of model initial conditions using satellite imagery. *Bull. Amer. Meteor. Soc.*, **60,** 206–211.
——, 1985: Synoptic features associated with Los Angeles tornado occurrences. *Bull. Amer. Meteor. Soc.*, **66,** 657–662.
——, 1988: Improving the watch/warning program through use of significant events data. Preprints, *15th Conf. Severe Local Storms,* Baltimore, Amer. Meteor. Soc., 165–168.
——, and C. A. Doswell III, 1982: High resolution diagnosis of instability using hourly surface lifted parcel temperatures. Preprints, *12th Conf. Severe Local Storms,* San Antonio, Texas, Amer. Meteor. Soc., 172–175.
Hart, J. A., and W. D. Korotky, 1991: The SHARP Workstation—v1.50. A skew T/hodograph analysis and research program for the IBM and compatible PC. User's Manual. NOAA/NWS Forecast Office, Charleston, WV, 62 pp.
Hirt, W. D., 1985: Forecasting severe weather in North Dakota. Preprints, *14th Conf. Severe Local Storms,* Indianapolis, Indiana, Amer. Meteor. Soc., 328–331.
Johns, R. H., 1982: A synoptic climatology of northwest flow severe weather outbreaks. Part I: Nature and significance. *Mon. Wea. Rev.*, **110,** 1653–1663.
——, 1984: A synoptic climatology of northwest flow severe weather outbreaks. Part II: Meteorological parameters and synoptic patterns. *Mon. Wea. Rev.*, **112,** 449–464.
——, 1993: Meteorological conditions associated with bow-echo development. *Wea. Forecasting,* (in press).
——, and W. D. Hirt, 1987: Derechos: Widespread convectively induced windstorms. *Wea. Forecasting,* **2,** 32–49.
——, and P. W. Leftwich, Jr., 1988: The severe thunderstorm outbreak of July 28–29 1986. A case exhibiting both isolated supercells and a derecho producing convective system. Preprints, *15th Conf. Severe Local Storms,* Baltimore, Amer. Meteor. Soc., 448–451.
——, and W. R. Sammler, 1989: A preliminary synoptic climatology of violent tornado outbreaks utilizing radiosonde standard level data. Preprints, *12th Conf. Wea. Analysis and Forecasting,* Monterey, California, Amer. Meteor. Soc., 196–201.
——, K. W. Howard, and R. A. Maddox, 1990a: Conditions associated with long-lived derechos—An examination of the large scale environment. Preprints, *16th Conf. Severe Local Storms,* Kananaskis Park, Alberta, Canada, Amer. Meteor. Soc., 408–412.
——, J. M. Davies, and P. W. Leftwich, 1990b: An examination of the relationship of 0–2 km AGL "positive" wind shear to potential buoyant energy in strong and violent tornado situations. Preprints, *16th Conf. Severe Local Storms,* Kananaskis Park, Alberta, Canada, Amer. Meteor. Soc., 593–598.
——, ——, and ——, 1993: Some wind and instability parameters associated with strong and violent tornadoes. Part II: Variations in the combinations of wind and instability parameters. *Proc. Tornado Symposium III,* C. Church, Ed., Amer. Geophys. Union, (in press).
July, M. J., 1990: Forcing factors in the violent tornado outbreak of May 5, 1989: A study of scale interaction. Preprints, *16th Conf. Severe Local Storms,* Kananaskis Park, Alberta, Canada, Amer. Meteor. Soc., 72–77.
Junker, N. W., J. E. Hoke, and R. H. Grumm, 1989: Performance of NMC's regional models. *Wea. Forecasting,* **4,** 368–390.
Kamburova, P. L., and F. H. Ludlam, 1966: Rainfall evaporation in thunderstorm downdraughts. *Quart. J. Roy. Meteor. Soc.*, **92,** 510–518.
Kelly, D. L., J. T. Schaefer, R. P. McNulty, C. A. Doswell III, and R. F. Abbey, Jr., 1978: An augmented tornado climatology. *Mon. Wea. Rev.*, **106,** 1172–1183.
——, ——, and C. A. Doswell III, 1985: The climatology of nontornadic severe thunderstorm events in the United States. *Mon. Wea. Rev.*, **113,** 1997–2014.
Knight, C. A., and P. Squires, Eds., 1981: *Hailstorms of the Central High Plains. Vol. 1: The National Hail Research Experiment.* Colorado Associated University Press, 282 pp.
Korotky, W., R. W. Przybylinski, and J. A. Hart, 1993: The Plainfield, Illinois tornado of August 28, 1990: The evolution of synoptic and mesoscale environments. *Proc., Tornado Symposium III,* C. Church, Ed., Amer. Geophys. Union, (in press).
Krumm, W. R., 1954: On the cause of downdrafts from dry thunderstorms over the plateau area of the United States. *Bull. Amer. Meteor. Soc.*, **35,** 122–126.
Lanicci, J. M., and T. T. Warner, 1991: A synoptic climatology of the elevated mixed-layer inversion over the southern Great Plains in spring. Part I: Structure, dynamics, and seasonal evolution. *Wea. Forecasting,* **6,** 181–197.
LaPenta, K. D., R. J. Kane, and J. S. Waldstreicher, 1990: A multiscale examination of the 10 July 1989 northeast tornado outbreak. Preprints, *16th Conf. Severe Local Storms,* Kananaskis Park, Alberta, Canada, Amer. Meteor. Soc., 548–553.
Lazarus, S. M., and K. K. Droegemeier, 1990: The influence of helicity on the stability and morphology of numerically simulated storms. Preprints, *16th Conf. Severe Local Storms,* Kananaskis Park, Alberta, Canada, Amer. Meteor. Soc., 269–274.
Leftwich, P. W., 1984: Operational experiments in prediction of maximum expected hailstone diameter. Preprints, *10th Conf. Wea. Forecasting and Analysis,* Clearwater Beach, Florida, Amer. Meteor. Soc., 525–528.
——, and S. K. Beckman, 1992: A preliminary assessment of the use of 404 MHz wind profiler data at the National Severe Storms Forecast Center. *J. Atmos. Oceanic Technol.,* (in press).
Lemon, L. R., and C. A. Doswell III, 1979: Severe thunderstorm evolution and mesocyclone structure as related to tornadogenesis. *Mon. Wea. Rev.*, **107,** 1184–1197.
Lewis, J., 1989: Real time lightning data and its application in forecasting convective activity. Preprints, *12th Conf. Wea. Analysis and Forecasting,* Monterey, California, Amer. Meteor. Soc., 97–102.
Lilly, D. K., 1986: The structure, energetics, and propagation of rotating convective storms. Part II: Helicity and storm stabilization. *J. Atmos. Sci.*, **43,** 126–140.
Maddox, R. A., 1976: An evaluation of tornado proximity wind and stability data. *Mon. Wea. Rev.*, **104,** 133–142.
——, 1993: The diurnal low-level wind oscillation and storm-relative helicity. *Proc., Tornado Symp. III,* C. Church, Ed., Amer. Geophys. Union, (in press).
——, and C. A. Doswell III, 1982: An examination of jetstream configurations, 500 mb vorticity advection and low-level thermal advection patterns during extended periods of intense convection. *Mon. Wea. Rev.*, **110,** 184–197.
——, L. R. Hoxit, and C. F. Chappell, 1980: A study of tornadic thunderstorm interactions with thermal boundaries. *Mon. Wea. Rev.*, **108,** 322–336.
McCaul, E. W., Jr., 1990: Simulations of convective storms in hur-

ricane environments. Preprints, *16th Conf. Severe Local Storms,* Kananaskis Park, Alberta, Canada, Amer. Meteor. Soc., 334–339.

——, 1991: Buoyancy and shear characteristics of hurricane-tornado environments. *Mon. Wea. Rev.*, **119,** 1954–1978.

McNulty, R. P., 1978: On upper kinematics and severe weather occurrence. *Mon. Wea. Rev.*, **106,** 662–672.

——, 1981: Tornadoes west of the divide: A climatology. *Natl. Wea. Dig.*, **6,** 2, 26–30.

Miller, R. C., 1972: Notes on analysis and severe storms forecasting procedures of the Air Force Global Weather Central. Tech. Rep. 200 (rev.), Air Weather Service, 181 pp.

Moller, A. R., C. A. Doswell, III, and R. Przybylinski, 1990: High precipitation supercells: A conceptual model and documentation. Preprints, *16th Conf. Severe Local Storms,* Kananaskis Park, Alberta, Canada, Amer. Meteor. Soc., 52–57.

Moore, J. T., and H. A. Elkins, 1985: A synoptic analysis of the 6–7 May 1975 Omaha tornado outbreak. *Natl. Wea. Dig.*, **10,** 1, 39–56.

——, and J. P. Pino, 1990: An interactive method for estimating maximum hailstone size from forecast soundings. *Wea. Forecasting,* **5,** 508–525.

Morgan, G. M., Jr., and P. W. Summers, 1986: Hailfall and hailstorm characteristics. *Thunderstorms: A Social, Scientific, and Technological Documentary. Vol. 2: Thunderstorm Morphology and Dynamics,* 2nd ed., E. Kessler, Ed., University of Oklahoma Press, 237–257.

Nelson, S. P., 1983: The influence of storm flow structure on hail growth. *J. Atmos. Sci.*, **40,** 1965–1983.

Nolen, R. H., 1959: A radar pattern associated with tornadoes. *Bull. Amer. Meteor. Soc.*, **40,** 277–279.

Ostby, F. P., 1992: Operations of the National Severe Storms Forecast Center. *Wea. Forecasting,* **7,** 546–563.

Piltz, S. F., 1992: Operational hourly helicity—An experiment. Southern Topics Technical Attachment SR/SSD 92-2, Southern Region Headquarters NWS, Ft. Worth, TX, 5 pp.

Pino, J. P., and J. T. Moore, 1989: An interactive method for estimating hailstone size and convectively-driven wind gusts from forecast soundings. Preprints, *12th Conf. Wea. Analysis and Forecasting,* Monterey, California, Amer. Meteor. Soc., 103–106.

Plummer, D. W., 1989: Diagnostic and forecast graphics products at NMC using high frequency model output. *Wea. Forecasting,* **4,** 83–89.

Prosser, N. E., and D. S. Foster, 1966: Upper air sounding analysis by use of an electronic computer. *J. Appl. Meteor.*, **5,** 296–300.

Przybylinski, R. W., 1988: Radar signatures associated with the 10 March 1986 tornado outbreak over central Indiana. Preprints, *15th Conf. Severe Local Storms,* Baltimore, Amer. Meteor. Soc., 253–256.

——, and D. M. DeCaire, 1985: Radar signatures associated with the derecho, a type of mesoscale convective system. Preprints, *14th Conf. Severe Local Storms,* Indianapolis, Indiana, Amer. Meteor. Soc., 228–231.

——, S. Runnels, P. Spoden, and S. Summy, 1990: The Allendale, Illinois tornado—January 7, 1989. One type of an HP supercell. Preprints, *16th Conf. Severe Local Storms,* Kananaskis Park, Alberta, Canada, Amer. Meteor. Soc., 516–521.

Rasmussen, E. N., and R. B. Wilhelmson, 1983: Relationships between storm characteristics and 1200 GMT hodographs, low-level shear, and stability. Preprints, *13th Conf. Severe Local Storms,* Tulsa, Oklahoma, Amer. Meteor. Soc., J5–J8.

Read, W. L., 1987: Observed microbursts in the NWS Southern Region during 1986—Four case studies. NOAA Tech. Memo. NWS SR-121. 10–34.

Rotunno, R., and J. B. Klemp, 1982: The influence of shear-induced vertical pressure gradient on thunderstorm motion. *Mon. Wea. Rev.*, **110,** 136–151.

——, and ——, 1985: On the rotation and propagation of simulated supercell thunderstorms. *J. Atmos. Sci.*, **42,** 271–292.

Schaefer, J. T., 1986: Severe thunderstorm forecasting: A historical perspective. *Wea. Forecasting,* **1,** 164–189.

Schmidt, J. M., and W. R. Cotton, 1989: A High Plains squall line associated with severe surface winds. *J. Atmos. Sci.*, **46,** 281–302.

——, C. J. Tremback, and W. R. Cotton, 1990: Numerical simulations of a derecho event: Synoptic and mesoscale components. Preprints, *16th Conf. Severe Local Storms,* Kananaskis Park, Alberta, Canada, Amer. Meteor. Soc., 422–427.

Scofield, R. A., and J. F. W. Purdom, 1986: The use of satellite data for mesoscale analyses and forecasting applications. *Mesoscale Meteorology and Forecasting,* P. S. Ray, Ed., Amer. Meteor. Soc., 118–150.

Smith, B. E., 1990: Mesoscale structure of a derecho-producing convective system: The southern Great Plains storms of May 4, 1989. Preprints, *16th Conf. Severe Local Storms,* Kananaskis Park, Alberta, Canada, Amer. Meteor. Soc., 455–460.

——, and J. W. Partacz, 1985: Bow echo induced tornado at Minneapolis on 26 April 1984. Preprints, *14th Conf. Severe Local Storms,* Indianapolis, Indiana, Amer. Meteor. Soc., 81–84.

Smull, B. F., and R. A. Houze, Jr., 1987: Rear inflow in squall lines with trailing stratiform precipitation. *Mon. Wea. Rev.*, **115,** 2869–2889.

Sohl, C. J., 1987: Observed microbursts in the NWS Southern Region during 1986—Four case studies. NOAA Tech. Memo. NWS SR-121, 1–9.

Srivastava, R. C., 1985: A simple model of evaporatively driven downdraft: Application to a microburst downdraft. *J. Atmos. Sci.*, **42,** 1004–1023.

Stone, H. M., 1988: Convection parameters and hodograph program -CONVECTA and CONVECTB. NOAA Tech. Memo. NWS ERCP No. 37 (revised), Eastern Region Headquarters, Bohemia, NY, 44 pp.

Szoke, E. J., and J. A. Augustine, 1990: A decade of tornado occurrence associated with a surface mesoscale flow feature—The Denver cyclone. Preprints, *16th Conf. Severe Local Storms,* Kananaskis Park, Alberta, Canada, Amer. Meteor. Soc., 554–559.

Turcotte, V., and D. Vigneux, 1987: Severe thunderstorm and hail forecasting using derived parameters from standard RAOB data. Preprints, *Second Workshop on Operational Meteor.,* Halifax, Nova Scotia, Canada, Atmos. Env. Serv./Canadian Meteor. and Oceanogr. Soc., 142–153.

Uccellini, L. W., 1990: The relationship between jet streaks and severe convective storm systems. Preprints, *16th Conf. Severe Local Storms,* Kananaskis Park, Alberta, Canada, Amer. Meteor. Soc., 121–129.

——, and D. R. Johnson, 1979: The coupling of upper and lower tropospheric jet streaks and implications for the development of severe convective storms. *Mon. Wea. Rev.*, **107,** 682–703.

Wakimoto, R. M., 1985: Forecasting dry microburst activity over the High Plains. *Mon. Wea. Rev.*, **113,** 1131–1143.

——, and J. W. Wilson, 1989: Non-supercell tornadoes. *Mon. Wea. Rev.*, **117,** 1113–1140.

Weisman, M. L., 1990: The genesis of bow echoes: A rear-inflow induced meso-convective structure. Cooperative Thesis No. 125, The Pennsylvania State University and National Center for Atmospheric Research. NCAR/CT-125, 149 pp.

——, and J. B. Klemp, 1984: The structure and classification of numerically simulated convective storms in directionally varying wind shears. *Mon. Wea. Rev.*, **112,** 2479–2498.

Weiss, S. J., 1987a: An assessment of the NGM four-layer lifted index prognoses of extreme instability. *Natl. Wea. Dig.*, **12,** 2, 21–31.

——, 1987b: Some climatological aspects of forecasting tornadoes associated with tropical cyclones. Preprints, *17th Conf. Hurr. and Trop. Meteor.*, Miami, Amer. Meteor. Soc., 160–163.

Wilson, J. W., J. A. Moore, G. B. Foote, B. Martner, A. R. Rodi, T. Uttal, and J. M. Wilczak, 1988: Convection Initiation and Downburst Experiment (CINDE). *Bull. Amer. Meteor. Soc.*, **69,** 1328–1348.

Woodall, G. R., 1990: Qualitative forecasting of tornadic activity using storm-relative environmental helicity. Preprints, *16th Conf. Severe Local Storms,* Kananaskis Park, Alberta, Canada, Amer. Meteor. Soc., 311–315.